# Regime shifts in satellite-derived chlorophyll within the Laurentian Great Lakes

Nikolay P. Nezlin[a,b]*, SeungHyun Son[a,c], Christopher W. Brown[a,b,c], Prasanjit Dash[a,d], Caren E. Binding[e], Ashley K. Elgin[f], Andrea VanderWoude[g]

[a] NOAA/NESDIS Center for Satellite Applications and Research, 5830 University Research Court, College Park, MD 20740, USA

[b] Global Science & Technology, Inc., 7501 Greenway Center Drive, Suite 1100, Greenbelt, MD 20770, USA

[c] Cooperative Institute for Satellite Earth System Studies (CISESS)/Earth System Science Interdisciplinary Center (ESSIC), University of Maryland, 5825 University Research Court College Park, MD 20742, USA

[d] Cooperative Institute for Research in the Atmosphere (CIRA), Colorado State University, 3925a Laporte Ave, Fort Collins, CO 80521, USA

[e] Environment and Climate Change Canada, Canada Centre for Inland Waters, 867 Lakeshore Road, Burlington, ON L7S 1A1, Canada

[f] NOAA Great Lakes Environmental Research Laboratory, Lake Michigan Field Station, 1431 Beach Street, Muskegon, MI 49441, USA

[g] NOAA Great Lakes Environmental Research Laboratory, 4840 S State Road, Ann Arbor, MI 48108, USA

*Corresponding author: nikolay.nezlin@noaa.gov; +1-(310)-770-1302

**Abstract**

As a result of implementation of nutrient management following the binational Great Lakes Water Quality Agreement in 1972, the ecosystems within the Laurentian Great Lakes were gradually transforming to lower trophic regimes. This transformation dramatically accelerated in the late 1980s after the introduction of two invasive species of filter-feeding mussels of the genus *Dreissena*. We performed a detailed analysis of spatial and temporal patterns of this transformation using remotely sensed surface chlorophyll-*a* concentration (*Chl-a*) from the multi-satellite long-term Ocean Colour Climate Change Initiative (OC-CCI) dataset as a proxy of ecosystem state. We analyzed 25 years (1997-2022) of monthly composites covering most of the Great Lakes' area detecting regime shifts in *Chl-a* employing an integrated approach combining Seasonal-Trend decomposition (STL) and Sequential T-test Analysis of Regime Shifts (STARS). The results identified the timings (shift points) when *Chl-a* stabilized at new lower trophic regimes, the magnitudes of *Chl-a* decrease across various lake regions and depths, and the changes in *Chl-a* seasonal cycles. In Lakes Michigan, Huron and Ontario, the timings and magnitudes of regime shifts and vanishing of spring phytoplankton bloom suggest that dreissenid mussel presence was a primary driving factor of the observed transformation. We demonstrate that the OC-CCI dataset is a reliable source of information that enables the detection of these regime shifts in major lakes, with only minor effects of inconsistencies resulting from the biases between different satellites collecting data during different time periods.

**Keywords:** Laurentian Great Lakes; Chlorophyll-*a*; Remote sensing; Regime shift; Dreissenid mussels; *Dreissena*

## 1. Introduction

Decreases in phytoplankton biomass and productivity in the Laurentian Great Lakes over the past decades demonstrate a cumulative effect of significant reduction of nutrient loads and the introduction of invasive species. Since European settlement through to the early 1980s, the Great Lakes experienced progressive eutrophication (Stoermer et al., 1990), with phosphorus as the major nutrient limiting primary production (Schelske et al., 1974). In response to the deteriorating state of water quality in these lakes, the binational Great Lakes Water Quality Agreement (GLWQA), a commitment between the US and Canada to provide a framework for identifying binational priorities to improve and protect water quality, was signed in 1972 (International Joint Commission, 1972). As a result of the control programs, phosphorus loadings to the lakes substantially decreased during the 1970s and 1980s (Bunnell et al., 2014), resulting in significant lake-wide reductions in phytoplankton biomass (Stevens and Neilson, 1987; Millard et al., 1996).

The decrease of phytoplankton biomass in the Great Lakes dramatically accelerated in the 1990s after the colonization of the lakes by two species of filter-feeding mussels: *Dreissena polymorpha* (Pallas, zebra mussel) and *D. rostriformis bugensis* (Andrusov, quagga mussel), hereafter referred to collectively as “dreissenids”. As suspension filter-feeders, the magnitude of their impact on pelagic ecosystems results from their ability to filter massive volumes of water (Kryger and Riisgård, 1988; Horgan and Mills, 1997; Diggins, 2001). A little selection of particle size or quality is performed during filtration, so more water is filtered than would be required to feed an individual, and not all filtered particles are consumed. Excess food and particles that are too large or are of low food quality are bound in mucus and expelled as pseudofeces (Padilla et al., 1996). As a result, these mussels affect pelagic ecosystems through both top-down control by feeding on planktonic organisms and bottom-up control by sequestering phosphorus that otherwise would be available to phytoplankton (Bunnell et al., 2014). The total impact of an individual mollusk on the planktonic community is, therefore, much greater than the impact of the same biomass of other predators (e.g., zooplankton).

The effect of zebra and quagga mussels on the Great Lake ecosystem included an increase in water transparency (Binding et al., 2015; Yousef et al., 2017; Son and Wang, 2019), a decrease in the biomass/abundance of phytoplankton and chlorophyll-*a* (Fahnenstiel et al., 2010; Vanderploeg et al., 2010; Reavie et al., 2014), decline in zooplankton (Kerfoot et al., 2010; Barbiero et al., 2011; Pothoven and Fahnenstiel, 2015; Kovalenko et al., 2018) and prey fish (Bunnell et al., 2014; Madenjian et al., 2015), and changes in the structure of the nearshore benthic community (Pillsbury et al., 2002; Hecky et al., 2004; Nalepa et al., 2009).

It is unclear whether the reduction in phytoplankton biomass and increase in water clarity result primarily from the regulation of nutrient discharge or the heterotrophic pressure of mussels on phytoplankton biomass plays a dominating role in the observed transformation in the Great Lakes. The effect of nutrient regulation is expected to result in a gradual decrease of phytoplankton biomass over most of the lakes' area. In contrast, the effect of mussel feeding is expected to be correlated with the steps of colonization of the lakes by dreissenids documented in previous studies (Nalepa et al., 2010, 2009; Karatayev and Burlakova, 2022; Karatayev et al., 2021).

The details of the transformation of the pelagic ecosystems of the Great Lakes to new lower trophic regimes are described in numerous publications based on field sampling (Fahnenstiel et al., 2010; Mida et al., 2010; Bunnell et al., 2014; Madenjian et al., 2015; Kovalenko et al., 2018; Pothoven and Vanderploeg, 2020) and satellite radiometry (Yousef et al., 2017, 2014; Rowe et al., 2015; Fahnenstiel et al., 2016; Son and Wang, 2020, 2019). Binding et al. (2015) used an empirical algorithm relating water clarity (Secchi disk depth) to reflectance measured in the green bands of Coastal Zone Color Scanner (CZCS), Sea-viewing Wide Field-of-view Sensor (SeaWiFS), and Moderate Resolution Imaging Spectroradiometer on Aqua platform (MODIS-Aqua), and showed a long-term increase (up to 62%) in water transparency comparable to the changes in *Chl-a* as reported in this study. However, most published results were focused either on separate lakes or over relatively short time periods, and many provided assessments averaged over an entire lake and/or depth zone. Furthermore, most published works conclude that this transformation is ongoing (Nalepa et al., 2010, 2009; Reavie et al., 2014; Rowe et al.,

2017, 2015). It is thus unknown if phytoplankton biomass has stabilized to new lower trophic regimes and what the final magnitude of that decrease was.

The questions of "when and where trophic status changes are occurring" can be addressed using estimates of surface chlorophyll-*a* concentration derived from visible measurements collected by Earth-observing satellites. Remotely-sensed water color represents a unique source of information for quantitative assessment of interannual variations of large-scale aquatic ecosystems (including ocean and large lakes), especially in the regions where detailed monitoring based on field surveys is unavailable (Calamita et al., 2024). However, combining the data collected by different satellites into one time series may introduce abrupt shifts and inconsistencies resulting from the differences in accuracy and resolution (spatial, temporal, and spectral) between satellite sensors.

The merged dataset produced by the Ocean Colour Climate Change Initiative (OC-CCI) project includes data corrected for the biases between the reflectances measured by different satellite sensors (Sathyendranath et al., 2019). The most recent version (v.6.0) of the OC-CCI dataset covers >25 years (1997-2022) of continuous global observations and can be used to analyze long-term interannual variations in different aquatic regions. It is important to keep in mind that the early stages of the oligotrophication process in the Great Lakes are not quantified in this study. The OC-CCI dataset started more than two decades after the beginning of nutrient discharge regulation and several years after the first reports of the introduction of dreissenids.

This study provides a detailed analysis of spatial and temporal variations of remotely-sensed chlorophyll-*a* concentration (*Chl-a*) in the five North American Laurentian Great Lakes (Superior, Michigan, Huron, Erie, and Ontario) using a consistent methodology for detecting regime shifts. We performed a quantitative assessment of regime shifts based on *Chl-a,* thus enabling estimation of the timing of shift points between the regimes and the differences between the mean levels of the regime indicator. The objectives of our study include: 1) addressing the question of whether the biases between the data collected during different periods by different satellites can be misinterpreted as regime shifts; 2) estimating the timings (shift points) when different regions of the lake ecosystems stabilized at new lower trophic

regimes; 3) quantifying the magnitudes of the *Chl-a* decrease in different geographic and bathymetric zones of the lakes; and 4) analyzing the effect of regime shift on *Chl-a* seasonal cycles in different parts of the lakes. The paper is organized as follows: Section 2 describes the study area; Section 3 describes the steps of colonization of dreissenids in the Great Lakes; Section 4 details the OC-CCI dataset and statistical methods of data processing and regime shift detection; Section 5 presents the results of the study, and is followed by discussions in Section 6 and conclusions in Section 7.

## 2. The study region: The Laurentian Great Lakes

The Laurentian Great Lakes (Figure 1) is one of the largest freshwater systems in the world, with a total lake surface area of 244,000 $km^2$ and a catchment area of approximately 1 million $km^2$. The lakes contain 22,000 $km^3$ of water, which is 84% of North America's surface fresh water and 21% of the world's surface fresh water supply (Sterner et al., 2017), with the lowest nutrient loads in mass per unit time entering Lake Superior and the largest nutrient load entering Lake Erie (Sterner, 2021). The Great Lakes basin is home to almost 40 million people, or roughly 10% of the US and 32% of Canada's population (Méthot et al., 2015). The lakes differ in size (from 18,960 $km^2$ for Lake Ontario to 82,100 $km^2$ for Lake Superior (Bunnell et al., 2014)), mean depth (from 7 m for western Lake Erie to 147 m for Lake Superior (Bunnell et al., 2014; Sterner, 2021)), hydraulic residence time (from about 200 years for Lake Superior to about three years for Lake Erie (Quinn, 1992)), and levels of primary production (from the ultra-oligotrophic Lake Superior to the periodically hypereutrophic waters of western Lake Erie (Bunnell et al., 2014; Dove and Chapra, 2015)).

Biogeochemical properties of the Great Lakes vary over a broad range of temporal and spatial scales (Sterner, 2021). Among the features potentially encouraging the colonization by dreissenids are relatively high pH and dissolved inorganic carbon (DIC) resulting from a high abundance of limestone and carbonate weathering in all lakes except for Lake Superior (Lin and Guo, 2016), a factor supporting the growth of invasive mussels (Hincks and Mackie, 1997). On

the other hand, a negative factor affecting benthic organisms is hypolimnetic hypoxia, which is a regular seasonal event in some shallow embayments (Sterner, 2021), as well as the central basin of Lake Erie, where hypoxia sometimes extended up to 60% of the surface area (Zhou et al., 2013). The spatial distribution of dreissenids in Lake Erie has been clearly connected to the occurrence of hypoxia (Karatayev et al., 2018b).

Because of their large size, the five lakes are often considered "inland seas", requiring a scientific approach with attributes similar to those of oceanography (Sterner et al., 2017). One of these approaches is using satellite remote-sensing imagery, providing regular synoptic coverage and the opportunity for comprehensive assessment of lake-wide water quality and robust determination of spatial and temporal trends (Binding et al., 2015).

## 3. Colonization of the Great Lakes by dreissenids

The introduction and expansion of zebra and quagga mussels in the Great Lakes has been well documented and represents one of the most dramatic and impactful colonizations of invasive species in modern times (Ricciardi and MacIsaac, 2000; Evans et al., 2011; Lower et al., 2024). These small (maximum size 50 mm) mollusks were introduced with the release of ballast waters from commercial vessels (Ricciardi and MacIsaac, 2000). The first occurrence of zebra mussels was noted between April and November 1986 in the western basin of Lake Erie (Carlton, 2008), followed by its formal (i.e., published) discovery on 1 June 1988 in Lake St. Clair, a small lake between Lakes Huron and Erie (Hebert et al., 1989). The zebra mussel extended its distribution beyond Lake Erie and was found in 1989 in three other lakes: Michigan, Huron, and Ontario (Griffiths et al., 1991; Karatayev et al., 2021). 1989 also marked the first record of the quagga mussel in North America when a single specimen was found in Lake Erie (Benson, 2014). The discovery of quagga mussels in Lake Ontario followed soon after in 1990 (Benson, 2014). In 1997, quagga mussels appeared in northern Lake Michigan and eastern Lake Huron (Karatayev et al., 2021). Zebra mussels and then quagga mussels were discovered in Lake Superior proper

in the early 2000's (Grigorovich et al., 2008, 2003), but marginal calcium levels have dampened their expansion (Trebitz et al., 2019).

The process of colonization and the dynamic between the two dreissenid species is influenced by how their differing physiologies react to environmental conditions. Zebra mussels have lower filtration rates (Diggins, 2001) and assimilation efficiencies (Baldwin et al., 2002), as well as higher respiration rates (Stoeckmann, 2003; Karatayev et al., 2015) when compared to quagga mussels. Quagga mussels are capable of spawning at colder temperatures (Roe and MacIsaac, 1997; Claxton and Mackie, 1998) and can adapt to soft substrate (Karatayev and Burlakova, 2022). Accordingly, zebra mussels are better equipped for warmer, more productive nearshore environments, while quagga mussels can readily inhabit cold, deep waters (Karatayev et al., 2015; Strayer et al., 2019).

Lake morphometry largely dictates the outcome of dreissenid mussel composition and distribution (Strayer et al., 2019; Karatayev et al., 2021). In shallow, productive regions such as the Western Basin of Lake Erie and Saginaw Bay in Lake Huron, zebra mussels peaked by the early 1990's and then have been able to persist after quagga mussels arrived, albeit at lower densities (Karatayev et al., 2021). In contrast, quagga mussels are competitively superior to zebra mussels in deeper, oligotrophic waters (Nalepa et al., 2010). In Lake Ontario, Lake Huron, and Lake Michigan, quagga mussels virtually displaced zebra mussels by 1997, 2003, and 2005, respectively, all within 8 years of their arrival (Karatayev et al., 2021). Further, the biomass attained by quagga mussels in these three lakes in 2018, 2017, and 2015 was more than ten times the maxima attained by zebra mussels in 1995, 2000, and 2000, respectively (Karatayev et al., 2022, 2021). As a result, the quagga mussel invasion waves caused stronger lake-wide ecosystem impacts compared to the more limited nearshore impacts of zebra mussels (Karatayev et al., 2022). The steps of colonization by both quagga and zebra mussels in shallow and deep basins of the Great Lakes are clearly illustrated in maps produced by Karatayev et al. (2021), which have been reproduced in Supplementary Figures S1a and S1b for ease of reference.

## 4. Data and Methods

### *4.1. Ocean Colour Climate Change Initiative (OC-CCI) dataset*

Surface chlorophyll-*a* concentration (*Chl-a*) is a proxy for phytoplankton biomass and one of the most widely used satellite ocean color products that are monitored by Earth-orbiting satellites (IOCCG, 2008). Multiple studies have used *Chl-a* to identify global trends and regime shifts in aquatic ecosystems (Behrenfeld et al., 2006; Chavez et al., 2011) and to monitor ecosystem health due to its direct link to aquatic net primary productivity and biomass (Wang and Convertino, 2023). Historical importance and availability of multi-decade *Chl-a* records motivated including it into the list of Essential Climate Variables (ECV), a limited set of variables deemed critical to the characterization of Earth's climate (GCOS, 2011; Bojinski et al., 2014).

The Ocean Colour Climate Change Initiative (OC-CCI) project of the European Space Agency (ESA) provides a consistent, long-term continuous dataset of merged ocean-color products created by integrating remote sensing reflectances (*Rrs*) from individual sensors (Table 1) and retrieving various ocean-color parameters via selected in-water algorithm (Lavender et al., 2015; Sathyendranath et al., 2019).

As different ocean color sensors often measure radiances at different wavebands, the input radiometric measurements were band-shifted to a common set of bands corresponding to the Medium Resolution Imaging Spectrometer (MERIS) on ENVISAT platform. The non-reference sensors of SeaWiFS, MODIS, VIIRS and OLCI (though OLCI already contains the MERIS bands so this was not required) were band shifted to the six main MERIS bands (412, 443, 490, 510, 560, 665nm) by computing Quasi-Analytical algorithm (QAA) (Lee et al., 2002) Inherent Optical Properties (IOP) and back computing the *Rrs* bands using a high-resolution spectral model (European Space Agency, 2022). Then, overlapping data were used to correct for mean biases between sensors, the corrected *Rrs* were merged by averaging all available data at every pixel with equal weight given to each available sensor, and the blended *Chl-a* algorithm (Jackson et al., 2017) was applied to the merged data to generate maps of chlorophyll concentration. The

merged products were validated against a global data set comprising *in situ* measurements collected from multiple sources (Valente et al., 2022).

Monthly *Chl-a* data at 4 km spatial resolution of the latest OC-CCI version 6.0 (September 1997–December 2022) were obtained from the OC-CCI dataset (https://climate.esa.int/en/projects/ocean-colour/).

In 2002, SeaWiFS had been operational for five years when MODIS-Aqua and MERIS were launched, and the total number of collected images dramatically increased. From 2012 to 2013, MERIS ceased operations, and Visible Infrared Imaging Radiometer Suite on the Suomi National Polar-orbiting Partnership platform (VIIRS -SNPP) was launched (Table 1). Starting in 2020, MODIS-Aqua and VIIRS-SNPP were not used in the OC-CCI dataset due to sensor degradation problems. Inter-mission differences in the merged OC-CCI *Chl-a* dataset may not have been completely corrected and may consequently be misinterpreted as trends and abrupt shifts (Mélin et al., 2017; Mélin, 2016; Hammond et al., 2018; Yu et al., 2023).

To evaluate if any spurious artifacts were introduced during merging, we compared OC-CCI *Chl-a* time series to the single-mission *Chl-a* time series of SeaWiFS, MERIS and MODIS-Aqua obtained from the Ocean Biology Processing Group at NASA Goddard Space Flight Center archive (https://oceandata.sci.gsfc.nasa.gov/). Monthly Level-3 Standard Mapped Image (SMI) *Chl-a* products with spatial resolutions at 4 km for MERIS (April 2002 to April 2012) and MODIS-Aqua (July 2002 to December 2022), and 9 km for SeaWiFS (September 1998 to December 2010) were examined. The *Chl-a* products in these datasets were derived using a combined *Chl-a* algorithm of OC3/OC4 (OCx) band ratio (O'Reilly and Werdell, 2019) and the color index (CI) algorithms (Hu et al., 2019). All satellite data were subsampled for the Great Lakes region (41.0-49.0N, 92.5-76.0W) and remapped with the standard cylindrical projection on 4-km resolution grids. For increased computational efficiency during statistical analysis, the resolution of all 4-km grids was reduced by a factor of three in each direction with a resulting cell represented as 3x3 median value (hereafter called 12-km grid cells).

Although many authors have questioned the absolute accuracy of the standard NASA *Chl-a* retrievals in the Great Lakes (Bergmann et al., 2004; Budd and Warrington, 2004; Watkins, 2009; Mouw et al., 2017, 2013; Moore et al., 2017; Sayers et al., 2019), other studies have indicated that the default iterative atmospheric correction is adequate for all the Great Lakes (Shuchman et al., 2013) and standard NASA band-ratio algorithms produce chlorophyll estimates that are linearly related to the *Chl-a* concentrations measured in the field (Lesht et al., 2013). Also, most of the areas analyzed in this study (excluding Lake Erie) are optically deep, therefore waters where the band-ratio method may be compromised by the presence of confounding substances (primarily embayments and shallow waters) constitute a comparatively small fraction of the Great Lakes (Lesht et al., 2013; Shuchman et al., 2013). Nevertheless, it is likely that increased uncertainty exists in the OC-CCI *Chl-a* particularly in turbid or eutrophic conditions and the nearshore, relative to other algorithms specifically tuned to optically complex waters. Utilizing the OC-CCI dataset for detecting regime shits in the Great Lakes' ecosystems, we therefore focus on relative temporal (interannual and seasonal) variations of remotely sensed *Chl-a* rather than assessment of the *Chl-a* absolute values.

### *4.2. Statistical methods of data analysis*

This study focused on quantitative analyses of the ecosystem's regime transformation in the Great Lakes, both from a whole lake and spatially explicit perspective. To quantify these changes, we applied the statistical method detecting a breakpoint between two periods: an early period characterized by a continuous stepwise decrease of *Chl-a* followed by a period of stable or increasing *Chl-a*. For this purpose, we selected the method that can evaluate two basic metrics of *Chl-a* decrease: 1) the timing (shift point) when the transformation from one regime to another is completed, and 2) the magnitude of this transformation (Figure 2c). The model is based on our understanding that oligotrophication was a dominant process over most of the Great Lakes. The selected model, however, may not apply to some regions for two reasons. First, some regions may not be affected by oligotrophication. Second, the process of regime transformation, which started in the late 1980s in some areas, could be completed earlier than

289 the OC-CCI dataset started in September 1997. The examples are Lake Superior, whose trophic
290 status did not change (Binding et al., 2015; Fahnenstiel et al., 2016), and Lake Erie, which has
291 undergone a period of re-eutrophication (Scavia et al., 2014; Watson et al., 2016).

292 The Sequential T-test Analysis of Regime Shifts (STARS; Rodionov, 2004) identifies timing(s)
293 when a system attribute – in our study, *Chl-a* – undergoes a persistent change. The basic
294 constraint regulating the durations of the detected regimes is the regimes cut-off length, the
295 parameter similar to the cut-off point in low-pass filtering. In this study, the regimes cut-off
296 length was determined through practical testing as 5 years (60 months). STARS sequentially
297 analyzes each observation in the time series by testing whether it is statistically different from
298 the current regime by calculating a Regime Shift Index (RSI) based on the Student's t-test to
299 confirm or reject the existence of a regime change (Rodionov and Overland, 2005; Rodionov,
300 2004). Many authors used this method for detecting abrupt changes in paleoecological records
301 (Espinoza et al., 2022), climate (Marty, 2008; Reid et al., 2016), marine ecosystems (Tian et al.,
302 2008; Conversi et al., 2010; Möllmann and Diekmann, 2012; Möllmann et al., 2009; Greene et
303 al., 2013) and many other studies.

304 Before applying STARS, seasonal variability was removed from each analyzed time series of *Chl-*
305 *a* using the Seasonal-Trend decomposition using LOESS (STL) method (Cleveland et al., 1990).
306 This filtering procedure decomposes a time series into the three components – trend, seasonal,
307 and remainder – by extracting smoothed estimates of each component using a locally
308 estimated scatterplot smoothing (LOESS) method based on local polynomial regressions. A
309 salient feature of STL is that it allows amplitude variation in the seasonal component for a given
310 period (e.g., annual), which helps capture a more significant portion of total variance than
311 amplitude alone (Vantrepotte and Mélin, 2009). We did not use the "pre-whitening" approach
312 recommended by Rodionov (2006) because preliminary analysis revealed that in the monthly
313 data examined, the components generated by stationary red noise processes were not
314 misinterpreted as "climatic regimes". Instead, we focused on removing seasonal variations,
315 which contributed substantially to the variability and hindered the identification of statistically
316 significant shift points. For this, each time series (an example in Figure 2a) was decomposed by

STL into trend (blue line in Figure 2c), seasonal (Figure 2b) and remainder (residual) components and then residuals were added to the trend, and the resulting "deseasonalized" time series (black line in Figure 2c) was analyzed by STARS. Each *Chl-a* time series was log-transformed prior to STL and STARS analysis and the outputs were inverse-transformed because the *Chl-a* values vary over several orders of magnitude and because log-transformed *Chl-a* is more normally distributed than the untransformed data (Campbell, 1995).

We applied the integrated STL-STARS algorithm to the time series of median *Chl-a* for individual lakes and each 12-km grid cell within each lake with at least 120 monthly observations, i.e., twice the regimes cut-off length, the parameter regulating minimum regime duration in STARS algorithm. In each location, transformation to a lower trophic regime was typically a gradual process that took several years and, as such, the STARS method detected a cascade of regime shifts (Figure 2c). For individual lakes and grid cells, the STARS method identified the timings when the cell experienced its 'initial' and 'final' decreasing regime shifts. The 'final' shift timing is when *Chl-a* stabilized (saturated) at its 'final' concentration, after which no other decreasing shift in *Chl-a* was detected. Two parameters were documented from the 'initial' and 'final' regimes: 1) the year of the 'final' regime shift, i.e., ecosystem stabilization (months were ignored); and 2) the magnitude of *Chl-a* decrease during the regime transformation, which was calculated as the percentage difference between the chlorophyll concentrations of the 'initial' and 'final' regimes (Figure 2c).

The relationship between detected regime shifts and lake depth was analyzed using bathymetric data of the Great Lakes obtained from the NOAA National Centers for Environmental Information (NCEI) Marine Geology and Geophysics online archive https://www.ngdc.noaa.gov/mgg/greatlakes. The grids of scale 1:250,000 were reprojected to 12-km resolution similar to the resampled OC-CCI and single-mission satellite data.

The annual cycles of monthly median *Chl-a* were examined in each location during the 'starting' (1998-2002) and 'ending' (2018-2022) five-year periods of the 25-year OC-CCI time series. The timings of *Chl-a* monthly maxima were estimated from the five-year medians of monthly medians either in entire lakes or in spatially explicit (i.e., 12-km grid cells) perspective during

the 'starting' and 'ending' five-year periods. The timings of monthly *Chl-a* maxima were computed using the "centroid" method to yield a center of gravity in polar coordinates. Using the center of gravity (and viewing the results in polar coordinates) is deemed a better estimate for this purpose than other estimates, such as a simple average or a center of gravity in linear coordinates (Colebrook, 1979; Edwards and Richardson, 2004; Meis et al., 2009). Figure 3 is an example of this estimation for the grid cell located farthest from shore in the southern part of Lake Michigan (Figure 1M). The center of gravity (Figure 3b) of maximum average monthly median *Chl-a* was estimated to be mid-March (month 3.5) for the period from 1998 to 2002 and late October (month 10.8) for the last 5-year period (2018-2022), which were similar though not exactly the same as the *Chl-a* maxima assessed visually (Figure 3a). It is worth mentioning that although we operate monthly data (i.e., the times are integers), the resulting assessments of the centers of gravity can include decimal fraction leading to conclusions at sub-monthly time scale.

## 5. Results

### *5.1. Inter-mission artifact or shift to a different trophic state?*

Although the potential of discontinuities of *Chl-a* (and other derived bio-optical properties) and incorrectly detecting them as regime shifts in *Chl-a* was higher when satellite sensors changed or merged (Supplementary Figure S2), the analysis of the individual mission *Chl-a* time series collected by the three satellites operating during the beginning of the observed period, i.e., SeaWiFS, MODIS-Aqua, and MERIS, and used in the creation of OC-CCI, revealed decreasing trends and successive regime shifts similar to those detected in the merged OC-CCI dataset. This is particularly evident in Lakes Michigan and Huron (Figure 4). Furthermore, in most time series collected by single satellite sensors, regime shifts were detected in 2005 (Figure 4), when sources of data from satellite sensors in OC-CCI dataset did not change (Supplementary Figure S2a).

As the trends and shifts observed in chlorophyll concentrations of the OC-CCI dataset are similar to those observed in the single satellite missions, we conclude that they are real and not artifacts introduced during the creation of the OC-CCI dataset.

### *5.2. Timings and magnitudes of regime shifts in Chl-a*

The median concentrations of *Chl-a* in Lakes Michigan, Huron, and Ontario gradually decreased during 1997-2012 (Figure 5). In Lakes Michigan and Huron, the integrated STL-STARS method detected a cascade of three regime shifts to a lower trophic state followed by a small shift to higher trophic state between 2014-2016 (Figure 5M, H). In Lake Ontario, a cascade of two regime shifts to lower trophic state was detected (Figure 5O). No decrease of *Chl-a* was observed in Lakes Superior and Erie (Figure 5S, E), though small but significant increases of *Chl-a* were detected in Lake Erie in 2002 and in Lake Superior in 2014.

The year when chlorophyll concentration reached its 'final' stable levels, i.e., *Chl-a* no longer declined, differed regionally within and between each of the Great Lakes (Figures 6 and 7). In Lakes Michigan, Huron, and Ontario, *Chl-a* decreased between 2002 and 2020 over most of the lake's areas. In Lake Superior, only the western portion of the lake experienced a decrease in *Chl-a* during the first decade of the observed OC-CCI time series (2002-2008; Figure 6S). The majority of Lake Erie also exhibited limited shifts in *Chl-a,* occurring along its western Canadian shore early in the OC-CCI time series and along the Michigan shore and in Lake St. Clair during the latter part of the dataset (Figure 6E). In Lake Huron, a lower trophic regime was achieved earlier (in 2002-2005) in the Georgian Bay than in the northeast, then in the southern and northwestern nearshore zones and along the Alpena-Amberley Ridge (marked in Figure 1H). Circa 2012, *Chl-a* decreased to its 'final' level in the remaining open parts of the lake (Figure 6H). Over most of Lake Ontario, the process to the new regime was slow. Over most of the lake, the *Chl-a* achieved a stable regime as late as 2015-2020 (Figure 6O). Only the small central-eastern region of the lake experienced the regime shift earlier (2002).

In Lake Michigan, the *Chl-a* level stabilized first in the nearshore regions north of 44°N (Figure 6M). From 2010 to 2012, a new regime was established offshore in the northern part of the lake and started spreading to its southern part, first along the western and eastern shores and then offshore. Offshore in the southern portion of the lake, the level of *Chl-a* stabilized as late as 2020.

Similar to the timing, the magnitude of the reduction in *Chl-a* between its 'initial' and 'final' stabilized concentrations also varied regionally within and between each of the Great Lakes. In Lakes Superior and Erie, where regime shifts were rarely found, the magnitudes of detected regime shifts were typically below 10% (Figure 7S, E). In Lake Michigan, *Chl-a* decreased 10-25% north of 44°N and 35-45% in the south (Figure 7M). Both the timing (Figure 6M) and magnitude of *Chl-a* decrease indicate that to the north of 44°N transformation of ecosystem from eutrophic to oligotrophic state started before the start of the OC-CCI dataset in 1997 and was completed few years earlier than in the south and a substantial part of this process was not captured in our analysis. In Lake Huron, the reduction in *Chl-a* varied between 20%-40%, with a maximum in its deeper southern portion (Figure 7H). Lastly, in Lake Ontario, the magnitude of *Chl-a* reduction was about 10% in the eastern part of the lake and 20-30% in its western part (Figure 7O).

The relationship between the timing (year) when *Chl-a* reached stable levels and lake bathymetry showed no apparent pattern (not shown), whereas the difference in its magnitude did (Figure 8). In Lake Superior, the difference in *Chl-a* between the 'initial' and 'final' regimes clearly decreased with increasing depth until it exceeded ~100 m. In Lakes Michigan and Huron, the lakes that exhibited the most evident regime shifts, the difference in *Chl-a* was most pronounced in water between 30 and 100 meters deep. No clear-cut relationship was observed in Lakes Erie and Ontario, the former likely due to its limited depth range.

### *5.3. Chlorophyll concentration phenology*

Analyzing seasonal cycles of *Chl-a* in the Great Lakes based on OC-CCI data, we have to bear in mind that the number of images collected during winter was much lower as compared to other seasons due to data gaps associated with cloud and ice coverage (see Supplementary Figure S3). The number of images acquired during December-January was low over all five lakes, especially over the Lakes Superior and Huron (Supplementary Figure S3S, H).

Significant changes in seasonal cycles of *Chl-a* over the entire lake areas were observed in Lakes Michigan (Figure 9M, 10M1, M2) and Huron (Figure 9H, 10H1, H2). In Lake Michigan during 1998-2002, two maxima of median *Chl-a* were observed in April-June and August (Figure 9M); the plot of the timings of *Chl-a* seasonal maxima demonstrates that these two maxima were observed in different parts of the lake: maximum in April-June in the southern part and maximum in August in the northern part (Figure 10M1). In 2018-2022, the timing of seasonal maximum changed to October over the entire lake (Figure 9M, 10M2). In Lake Huron during 1998-2002, the median (averaged over the entire lake) *Chl-a* maximum was in winter-spring (March-June; Figure 9H); a spatially explicit view revealed winter maximum in nearshore parts of the lake and spring maximum in open waters (Figure 10H1). By 2018-2022, the timing of seasonal maximum changed to fall (October-December). In both Lakes Michigan and Huron, the changes in the timings of seasonal maxima occurred between 2002 and 2004 (Figure 9a).

We speculate that a seasonal maximum in the northern Lake Michigan may not have been observed in spring (in contrast to its southern part; Figure 10M1) because, during the beginning of the OC-CCI dataset, local ecosystems had already undergone most, if not all of the regime transformation. This explanation agrees with early stabilization and low magnitude of regime shifts observed there (Figures 6M and Figure 7M).

In Lake Superior, the timing of *Chl-a* maximum (October-December) did not change, but its magnitude substantially decreased (Figure 9S, O). The differences in the timing and magnitude of winter maximum in Lake Superior in 1998-2002 (fall maximum in its northern part and winter maximum in the south; strong maximum in 1998-2002 vs. small maximum in 2018-2022) can be attributed to flaws in OC-CCI data resulting from very low number of satellite images acquired

over Lake Superior during winter seasons 1998-2002 when the maxima were detected and only one satellite (SeaWiFS) collected data.

In Lake Erie, *Chl-a* maximum in 1998-2002 was observed in winter (Figure 10E1), and its timing did not change by the end of the observed period (Figure 10E2). Similarly, in Lake Ontario, the timing of *Chl-a* summer maximum remained unchanged (June-September; Figure 9O, 10O1, O2).

During the 'ending' (2018-2022) 5-year period, we see an almost complete disappearance of a spring bloom, typical of temperate waters, replaced with an autumn bloom. In 2018-2022, seasonal *Chl-a* cycles in four lakes (Superior, Michigan, Huron, and Ontario) were characterized by a maximum in late fall (October-December; Figure 10S2, M2, H2, O2). The vanishing of spring maxima can be explained by the strong effect of mussel filtration on phytoplankton in the entire water column, including the near-surface layer, during spring when the water column is well mixed (see details in Discussion).

## 6. Discussion

To our knowledge, this is the first study to analyze a relatively long-term continuous and internally consistent time series of satellite-derived chlorophyll concentration to identify statistically significant, abrupt changes of chlorophyll concentration in a spatially explicit manner in all of the Laurentian Great Lakes during the same period. This approach permits us to examine inter- and intra-lake differences in the timing and magnitude of changes in chlorophyll concentration, and explore potential factors related to these changes.

### *6.1. Transformations to lower trophic regimes in the Great Lakes*

The spatial and temporal features of regime transformation in the Great Lakes described in this paper agree with the previously published information about the proliferation of dreissenid

mussels, supporting the hypothesis that colonization of the lakes by dreissenids was a primary driver of this transformation. A shift to the lower trophic state was evident in three initially mesotrophic deep lakes (Michigan, Huron, and Ontario) and small or absent in the consistently oligotrophic Lake Superior and regionally eutrophic Lake Erie. These results do not deny the role of nutrient management in improving water clarity in the Great Lakes, but indicate that mussel presence was an important driving factor of this oligotrophication.

*6.1.1. Lake Superior*

The magnitudes of regime shifts detected in Lake Superior were small compared to the other three deep lakes (Michigan, Huron, and Ontario). These assessments agree with the information that dreissenid mussels invaded Lake Superior in very low numbers (Grigorovich et al., 2008; Karatayev and Burlakova, 2022). Also, even before the dreissenid invasion, Lake Superior was characterized as the clearest of the Great Lakes, in terms of water transparency (Binding et al., 2015), phytoplankton/chlorophyll/primary production (Vollenweider et al., 1974) and zooplankton biomass (Barbiero et al., 2012). As a result, no differences between pre-mussel and post-mussel periods were found in water clarity (Binding et al., 2015; Yousef et al., 2017), phytoplankton (Reavie et al., 2014; Kovalenko et al., 2018), zooplankton (Kovalenko et al., 2018), chlorophyll (Barbiero et al., 2012; Fahnenstiel et al., 2016), and total phosphorus concentrations (Bunnell et al., 2014).

At the same time, small magnitudes of regime shifts detected in Lake Superior may be a result of less accurate (as compared with other deep lakes) *Chl-a* detection by the algorithms utilized in OC-CCI dataset. Mouw et al. (2017, 2013) indicated that in Lake Superior band-ratio algorithms significantly overestimate *Chl-a* because light absorption in its waters is dominated by CDOM, while very small contribution of phytoplankton and non-algal particles to overall absorption poses a challenge to deriving these parameters from reflectance spectra (Mouw et al., 2017, 2013), making the conclusions about temporal (seasonal and interannual) variations of *Chl-a* in that lake less reliable.

Recent observations in western Lake Superior documented cyanobacterial blooms in the narrow nearshore zone, a phenomenon never observed before 2012 (Sterner et al., 2020). These blooms may result in a positive regime shift in median *Chl-a* averaged over the entire lake including the nearshore (Figure 5S). Some authors attribute these recent changes in Lake Superior to atmospheric and lake warming (Reavie et al., 2014) extending its short (as compared to other lakes) period of summer stratification (Fahnenstiel et al., 2016).

### *6.1.2. Lake Michigan*

The details of regime transformation revealed by our spatially explicit analysis agree with the introduction and spread of dreissenids described in numerous publications (Nalepa et al., 2010, 2009; Evans et al., 2011; Madenjian et al., 2015; Rowe et al., 2015). Specifically, a significant number of dreissenids were first recorded in the northern nearshore regions in about 2000. By 2005, they had spread to the south nearshore, and by 2010, they had colonized offshore regions that resulted in a decrease in phytoplankton/chlorophyll biomass and an increase in water clarity. By 2015, however, maximum concentrations of dreissenids in the shallow regions slightly decreased (from $10^4$-$10^5$ to $10^3$-$10^4$ mussels $m^{-2}$ (Karatayev et al., 2021)).

In the northern basin, Reavie et al. (2014) noted that a decline in spring phytoplankton occurred by 2002, followed by no statistically significant long-term trend, while in the southern basin, a significant drop in phytoplankton biovolume occurred between 2004 and 2005. Fahnenstiel et al. (2010) demonstrated in the southern basin small or no decreases in *Chl-a*, phytoplankton biomass, and water column primary productivity between 1983–1987 and 1995–1998, followed by their substantial decrease by 2007–2008. In the same area, *Chl-a* decreased by 50% between 1995–2000 and 2007–2011 (Pothoven and Fahnenstiel, 2013). Yousef et al. (2017, 2014) reported a decrease in the diffuse attenuation coefficient (a proxy of water clarity based on SeaWiFS and MODIS-Aqua ocean color data) during 1998-2012 in the central part of the southern basin and no changes in the northern part of the lake. At the same

time, Sayers et al. (2020) found no increasing or decreasing linear trends in remotely-sensed *Chl-a* in all five Laurentian Great Lakes during 2003-2018.

Comparison between the results mentioned above and our assessments demonstrate the advantage of the approach used in this study, i.e., detecting a breakpoint between a decreasing trend followed by a stable regime, over the trend-detection method based on a linear model. The latter approach revealed significant changes in water clarity only in the offshore southern basin where, according to our results, *Chl-a* was decreasing during most of the OC-CCI period. Also, no linear trend was detected in the northern part of the lake and in the southern basin nearshore, where, according to our results, transformation took place during the initial part of the observed period until a stable regime was achieved.

### *6.1.3. Lake Huron*

Lakes Huron and Michigan experienced significant expansion of dreissenid populations, so it is not surprising that there are some similarities in their phytoplankton changes (Reavie et al., 2014). Previous studies documented a significant increase in water clarity associated with the deepening of the mean euphotic depth (from 41 m in 1998-2002 to 51 m in 2003-2010), which continued increasing in deeper (>30 m) regions (Yousef et al., 2017). In 2003, a dramatic reduction in the size of the spring phytoplankton maximum was reported in the entire lake (Barbiero et al., 2011; Reavie et al., 2014).

The decline in Lake Huron's spring phytoplankton biovolume occurred earlier and was more severe than that in Lake Michigan despite a faster and more abundant dreissenid invasion in the latter (Reavie et al., 2014). One possible reason for a lower density of mussels having a larger impact is that Lake Huron had a lower phytoplankton abundance prior to quagga mussel colonization and it is shallower than Lake Michigan (Yousef et al., 2017).

### *6.1.4. Lake Erie*

Lake Erie is very different from other Great Lakes in terms of its shallow bathymetry (mean depth 7 m to 24 m from west to east (Bunnell et al., 2014)), mineral turbidity, and high bioproductivity, especially in its western basin (Vollenweider et al., 1974; Reavie et al., 2014; Allinger and Reavie, 2013). No regime shift to lower trophic state was detected in that lake. Several studies documented a significant decrease in phytoplankton/chlorophyll concentration in some regions of Lake Erie within a few years of the establishment of large populations of zebra mussels (Holland, 1993; Makarewicz et al., 1999; Nicholls et al., 1999; Allinger and Reavie, 2013), yet this transformation may have occurred prior to the period comprising the OC-CCI dataset and hence could not be detected in this study.

During the two most recent decades of the OC-CCI time series examined, phytoplankton biomass in Lake Erie remained high and even increased, attributable primarily due to blooms of blue-green algae (cyanobacteria) observed in both nearshore and open parts of the lake (Twiss et al., 2012; Reavie et al., 2014; Yuan et al., 2021). These blooms can be explained by increasing phosphorus loading to the western basin resulting in re-eutrophication of the lake (Michalak et al., 2013; Scavia et al., 2014; Watson et al., 2016). These blooms dramatically compromise optical signal, because cyanobacteria often exhibit unique backscatter and absorption features due to the presence of gas vacuoles, variable pigmentation, or colonial aggregation into floating mats (Moore et al., 2017; Binding et al., 2019). These unique optical properties lead to several-fold underestimation of *Chl-a* by standard blue to green ratio-based algorithms (Stumpf et al., 2016, 2012; Binding et al., 2019; Wynne et al., 2021), especially during summer when blooms are most abundant (Wynne and Stumpf, 2015; Stumpf et al., 2012; Son and Wang, 2019). The peak chlorophyll observed in winter in this study is nevertheless in agreement with the extremely high biomass diatom blooms observed in Lake Erie during the winter (Binding et al., 2012b; Twiss et al., 2012), outside of the summer cyanobacteria bloom monitoring period typically reported on using satellite observations of the lake. However, given the known uncertainties of ratio-based *Chl-a* retrieval algorithms in highly turbid waters, the seasonal cycles of *Chl-a* obtained by the OC-CCI products may also reflect seasonal variability in mineral sediments rather than chlorophyll concentration (Binding et al., 2019, 2012a) with maximum in winter and minimum in summer. It is therefore important to consider further year-round

583 validation of the OC-CCI *Chl-a* retrievals in these optical extremes in order to provide
584 confidence in results in the case of the turbid eutrophic waters of Lake Erie.

585

586 *6.1.5. Lake Ontario*

587 Over most areas of Lake Ontario, the process of transformation to lower trophic regime
588 detected by the integrated STL-STARS method continued until the end of the OC-CCI dataset
589 (2020-2022). These assessments are corroborated by the conclusion that colonization of Lake
590 Ontario by dreissenid mussels was slow as compared to the other Great Lakes. One reason
591 could be that a high proportion of Lake Ontario is deep (>90 m) and mussels at greater depths
592 exhibit very slow growth rates (Elgin et al., 2022b). Karatayev et al. (2022) noted that the lake-
593 wide biomass of dreissenids continued increasing since its arrival (1989 for zebra mussels and
594 1990 for quagga mussels) and reached an all-time high in 2018 (the most recent whole-lake
595 data available at this time). Our assessments agree with the conclusion of Karatayev et al.
596 (2022) that the ecological effects of quagga mussels in Lake Ontario will likely continue into the
597 foreseeable future.

598 A slow rate of regime transformation in Lake Ontario detected by the integrated STL-STARS
599 method applied to OC-CCI data agrees with the data reported by Reavie et al. (2014), who
600 noted little overall change in total algal abundance during 2001-2011 with some changes taking
601 place in the composition of the phytoplankton assemblages.

602

603 *6.2. Effect of dreissenid filtration in different depth zones*

604 This study supports the hypothesis that the impact of dreissenid filter-feeding on pelagic
605 ecosystems depends on lake bathymetry, and this effect is nonlinear, with a maximum in the
606 mid-depth range (about 30-100 m) and a smaller effect in shallower and deeper waters. Similar
607 conclusions were reached earlier by several studies using a variety of approaches: by
608 Vanderploeg et al. (2010), estimating the clearance rates of quagga mussels; by Kerfoot et al.

609 (2010) and Yousef et al. (2014) from their assessments of decreasing rates of remotely-sensed
610 *Chl-a* in southern Lake Michigan; and by Karatayev and Burlakova (2022) in their review of
611 dreissenid mussel biology in the Great Lakes.

612 The comparatively small impact of dreissenid mussels in the shallow zone is explained by their
613 lower density resulting from unstable sandy substrate, physical disturbance by waves and
614 currents, thermal instability, and fish predation (Nalepa et al., 2010; Vanderploeg et al., 2010;
615 Glyshaw et al., 2015).

616 In deeper waters, the impact of dreissenid mussels on phytoplankton biomass is reduced by
617 vertical extension of the water column, i.e., greater biomass of dreissenids is required to filter
618 the same fraction of the water column due to greater volume per unit bottom habitat, and
619 slower rates of mussel filtration associated with low temperature and limited food availability.
620 At temperatures typical of shallow water, the filtration rates of dreissenids measured in
621 experiments achieved 400 mL $h^{-1}$ $mussel^{-1}$ (about 10 L $day^{-1}$ $mussel^{-1}$) (Kryger and Riisgård,
622 1988; Horgan and Mills, 1997; Diggins, 2001). However, the filtration activity of mussels
623 significantly (2- to 10-fold) decreases at lower temperatures (Vanderploeg et al., 2010; Xia et
624 al., 2021), reducing the volume of food consumed by mussels. Low food concentrations also
625 negatively affect dreissenid filtering activity (Malkin et al., 2012; Karatayev et al., 2018c; Xia et
626 al., 2021). Furthermore, during summer, the upper euphotic layer where phytoplankton is
627 concentrated is isolated by seasonal stratification from the hypolimnion affected by mussel
628 filtration. The effect of thermal stratification limiting the impact of filtration by benthic
629 organisms on the pelagic community in the Great Lakes was highlighted by several authors
630 (Fahnenstiel et al., 2010; Vanderploeg et al., 2010; Malkin et al., 2012; Karatayev et al., 2021).

631 Although the filter-feeding activity of dreissenids is most prominent in the mid-depth zone, it
632 also impacts offshore regions by reducing the amount of phytoplankton biomass transported
633 from the nearshore zone (Hecky et al., 2004; Kerfoot et al., 2010; Pothoven and Vanderploeg,
634 2020; Vanderploeg et al., 2010), where phytoplankton growth is stimulated by seasonal
635 tributary inputs and resuspension of nutrients (Vanderploeg et al., 2007; Johengen et al., 2008;
636 Rowe et al., 2017). At the beginning of regime transformation, dreissenids were concentrated

637 in the shallow zone and nutrients (primarily phosphorus) from allochthonous sources were
638 retained in the nearshore, thus impacting offshore pelagic communities through “nearshore
639 phosphorus shunt” (Hecky et al., 2004). The shift in the bulk of mussels from the nearshore to
640 the mid-depth zone (30-50 m) resulted in the fraction of the water column cleared at mid-
641 depth greatly exceeding phytoplankton growth, while the rates of seston uptake nearshore and
642 offshore were lower (Vanderploeg et al., 2010). This pattern of seston uptake at different
643 depths affected not only the mid-depth region, but also the offshore region “downstream” of
644 the mid-depth zone, suggesting a new “mid-depth carbon and phosphorus sink” hypothesis
645 (Vanderploeg et al., 2010). Further expansion of mussels to deep regions and declining density
646 and biomass in the shallowest zone resulted in the “offshore carbon and phosphorus sink”
647 hypothesis (Karatayev and Burlakova, 2022).

648

649 *6.3. Effect of dreissenids filtration on phytoplankton phenology (seasonal cycles)*

650 The disappearance of spring *Chl-a* maximum in Lakes Huron and Michigan corresponds closely
651 with the dreissenid invasion, and argues strongly for top-down control through filtration.
652 Bottom-up control through the reduction of nutrient input from the watershed and its
653 sequestration nearshore may have contributed to this, as well as climate changes, though we
654 cannot ascertain this in our study.

655 Climate change is an important factor affecting aquatic food webs (Edwards and Richardson,
656 2004; Behrenfeld et al., 2006; Adams et al., 2022); however, the timings of ecosystem
657 transformations observed in the Great Lakes do not appear to be a direct consequence of
658 global warming. Although previous studies indicated that since 1985 water temperature in the
659 Great Lakes was increasing even more rapidly than regional air temperature (Austin and
660 Colman, 2008; Schneider and Hook, 2010; O'Reilly et al., 2015), most abrupt warming occurred
661 from 1997 to 1998 (Van Cleave et al., 2014; Gronewold et al., 2015; Zhong et al., 2016), i.e., in
662 the beginning of the period analyzed in this study. The 1997/1998 warming started with an
663 anomalously warm El Niño winter over the northern US (Assel et al., 2000; Kumar et al., 2001)

664 followed by a long-term shift toward a negative phase of the Pacific Decadal Oscillation (PDO)
665 associated with an abnormally cold eastern Pacific Ocean and warm western-central North
666 Pacific Ocean (Mantua et al., 1997; Zhang et al., 1997; Newman et al., 2016).

667 Warming of the upper layer results in an earlier onset of springtime stratification in the Great
668 Lakes (Zhong et al., 2016; Fichot et al., 2019; Calamita et al., 2021; Kayastha et al., 2023).
669 Under pressure by dreissenid mussels, the role of seasonal stratification is different from the
670 role it usually plays in phytoplankton phenology. Typically, stratification retains phytoplankton
671 cells in the euphotic zone where production by photosynthesis is balanced by loss processes,
672 sinking and heterotrophic grazing. With shallowing of the seasonal thermocline in spring,
673 phytoplankton receive more solar energy while nutrient concentrations are still high; as a
674 result, photosynthetic growth exceeds loss processes producing a spring ('vernal')
675 phytoplankton bloom (Sverdrup, 1953; Siegel et al., 2002). In the regions where the abundance
676 of filter-feeding mussels is high and the water column is well mixed (e.g., in winter-spring
677 before the formation of seasonal thermocline), intensive heterotrophic pressure in the near-
678 bottom layer reduces net primary production in the entire water column and, as a result, a
679 spring maximum is not formed (Fahnenstiel et al., 2010; Kerfoot et al., 2010; Vanderploeg et al.,
680 2010; Reavie et al., 2014; Rowe et al., 2015).

681 In summer, when nutrients in the upper mixed layer are depleted, the thermocline plays the
682 role of a barrier between the subsurface euphotic layer and deep waters rich in nutrients, often
683 resulting in the formation of deep chlorophyll maximum (DCM), regularly observed in the Great
684 Lakes (Fahnenstiel and Scavia, 1987; Barbiero and Tuchman, 2004; Malkin et al., 2012; Scofield
685 et al., 2020; Fraker et al., 2021). With seasonal decrease in solar heating, erosion of the
686 thermocline increases nutrient supply to the upper mixed layer resulting in autumn
687 phytoplankton maximum observed in remotely-sensed *Chl-a* imagery. However, in the waters
688 affected by dreissenids, summer stratification not only retains photosynthetic algae in the
689 euphotic layer and controls vertical nutrient flux but also separates phytoplankton from benthic
690 filter-feeders (Fahnenstiel et al., 2010; Rowe et al., 2017, 2015; Karatayev et al., 2021, 2018a).

As such, erosion of stratification is expected to produce both positive (by nutrient supply) and negative (by grazing) effects on phytoplankton dynamics.

It is unclear why in the Great Lakes, in fall, when the seasonal thermocline is eroding, a positive effect of nutrient flux to the euphotic zone outweighs the negative effect of filter-feeders. A possible explanation is that an increase of near-surface *Chl-a* concentration in fall may result from shoaling DCM rather than phytoplankton growth associated with increased nutrient flux to the euphotic layer.

### *6.4. OC-CCI dataset as a source for regime shifts detection*

The OC-CCI *Chl-a* dataset appears to be a suitable source of information for detecting trends and regime shifts in aquatic regions when transformations are as dramatic as those observed in the Great Lakes. This is corroborated by Henson et al. (2016, 2010), who estimated that the minimum length of a time series required to detect *Chl-a* trends in the open ocean was 15-60 years based on the amplitude of trend to natural variability. The present duration of the OC-CCI dataset (25 years) is clearly within these limits and the magnitude of observed changes in *Chl-a* are much larger than those in the open ocean driven by global warming.

Unfortunately, the OC-CCI dataset only begins in 1997 when regular satellite-derived estimates of *Chl-a* are available and we are unable to analyze changes in *Chl-a* during the previous two decades when nutrient discharge regulation began and before the dreissenid mussel invasion in the Great Lakes started in 1988. Previous studies based on reflectances measured by satellite sensors operating during that period, such as the Advanced Very High Resolution Radiometer (AVHRR, operating since 1981) and Coastal Zone Color Scanner (CZCS; 1978-1986) demonstrated a significant increase in water clarity of the Great Lakes (Budd et al., 2001; Binding et al., 2015). Unfortunately, estimates of *Chl-a* from AVHRR imagery used by Budd et al. (2001) are unreliable because it does not possess the required wavebands used to derive *Chl-a*; it possesses only one visible (630 nm) channel (Stumpf and Pennock, 1991,1989; Woodruff et al., 1999). The “proof-of-concept” CZCS mission (1978-1986) onboard the Nimbus-

7 satellite was focused on estimates of ocean color, including assessments of *Chl-a* (Hovis et al., 1980). However, the attempts to compare *Chl-a* derived from CZCS to the more recent dedicated ocean color sensors resulted in ambiguous conclusions (Gregg et al., 2003; Antoine et al., 2005; Martinez et al., 2009) and the lack of overlap between CZCS and SeaWiFS prevented including CZCS in the OC-CCI *Chl-a* time series.

Other merged ocean color satellite datasets are available and could potentially be used to detect *Chl-a* trends. Of these, the most prominent is the Copernicus Marine Environmental Monitoring Service (CMEMS) GlobColour processor (Maritorena et al., 2010; Garnesson et al., 2019) where the continuous data set of *Chl-a* was generated by combining *Chl-a* products computed for each sensor using different algorithms. We chose not to use the GlobColour dataset because it was not explicitly bias-corrected and revealed higher discontinuities as compared with OC-CCI (Hammond et al., 2018).

OC-CCI is a developing project whose future versions will comprise additional satellite information, including reprocessed VIIRS SNPP after 2020, and two new VIIRS sensors onboard NOAA-20 (launched November 2017) and NOAA-21 (launched November 2022). These and other datasets with improved correction of inter-mission differences (Yu et al., 2023) will provide advanced possibilities to detect trends and regime shifts in different aquatic regions effectively.

### *6.5. Potential Issues*

We cannot be entirely certain that all biases introduced by the merging of observations collected by different satellite sensors were completely removed from the OC-CCI *Chl-a* dataset and hence could be misinterpreted by the STARS method as regime shifts. Yet any artifacts resulting from the compilation are likely minimal and did not affect the assessments of the timings and magnitudes of this transformation; the same trends and timing of shifts in chlorophyll concentration observed in the individual sensor data were also detected in the OC-CCI dataset.

Overall, we think that STARS is a good and appropriate method to detect and quantify the timings of regime shifts. We assume the regime cut-off length parameter we set to 5 years (60 months) was sufficient. Stirnimann et al. (2019), using the experiments with synthetic time series including artificial change points (APs), demonstrated that STARS detected regime shifts within a temporal range of ±12 time units (months) from (typically 1-3 time units before) AP and recommended caution to be used in the intra-annual (phenological scale) interpretations of the results when monthly time series is used. This recommendation agrees with the accuracy we used in this study, analyzing the calendar years of regime shifts and ignoring the months.

As stated previously, though we analyzed the longest time series of *Chl-a* currently available, the lakes have undoubtedly undergone changes prior to the 25 years comprising the OC-CCI dataset. For instance, the oligotrophication in lakes may have begun and ended earlier than the first year of the OC-CCI dataset, i.e., 1997. Furthermore, the monthly resolution of the OC-CCI will not capture details of short-lived events. Yet, for the purposes of this study, it provides a synoptic view at a sufficient temporal scale to document the mean environment and its changes over a year.

Another issue related to the application of OC-CCI dataset to nearshore shallow parts of the Great Lakes is that OC-CCI was not well calibrated for turbid shallow waters. Field samples for OC-CCI calibration were collected over depths >50 m (Sathyendranath et al., 2019). Similarly, the adopted *Chl-a* retrieval algorithm (a blended combination of the OC band ratio and color index) is optimized for both low *Chl-a* and typically Case-1 waters, where phytoplankton dominates the optical properties, and has been shown to carry larger uncertainties in optically complex Case-2 waters such as observed in Lake Erie (Binding et al., 2019). The ratio between total suspended solids (TSS) and *Chl-a* in Lake Erie is also higher than in other Great Lakes (Xu et al., 2022), making the assessments of remotely-sensed *Chl-a* less reliable. This kind of product uncertainty may contribute to the result that no regime shifts were detected in Lake Erie.

## 7. Conclusions

772 The results of this study demonstrate that the combined effect of regulation of nutrient loads
773 enhanced by the invasion of non-native filter-feeding mussels affected the ecosystems of the
774 Great Lakes differently. In two of the five lakes (deep, cold and already oligotrophic Lake
775 Superior and shallow eutrophic Lake Erie), the regime shift was either small, not detectable due
776 to uncertainties of algorithm performance in those optical water types, or completed before
777 1997, outside the temporal coverage of the analyzed time series. Over most of Lakes Michigan
778 and Huron, pelagic ecosystems stabilized at a new lower trophic regime from 2005–2015. In a
779 few locations (the central part of Lake Michigan, Saginaw Bay in Lake Huron, and most of Lake
780 Ontario), regime transformation either occurred prior to the timeframe of this study or is
781 ongoing and may continue in the future. The last few rounds of whole lake benthic surveys
782 have shown that dreissenid mussels have stabilized in many locations in the Great Lakes (Elgin
783 et al., 2022a). However, it is still unclear how the dreissenid populations will progress in these
784 areas and what changes in the community structure and functioning are expected in the future.

785 This study proves that inconsistencies in the OC-CCI dataset resulting from the biases between
786 different satellites collecting data during different periods are minor compared to regime
787 transformations observed in the Great Lakes during the recent two and a half decades. Given
788 that so far only 9% of the studies focused on regime shifts in lakes use satellite data as main
789 data source (Calamita et al., 2024), this study demonstrates that the OC-CCI dataset is a reliable
790 source of data that enables the detection of regime shifts in different regions of the world,
791 including major lakes.

792

793 **Data and Software Availability**

794 OC-CCI data are available from https://climate.esa.int/en/projects/ocean-colour/. Single-
795 mission satellite data of SeaWiFS, MERIS, and MODIS-Aqua are available from
796 (https://oceandata.sci.gsfc.nasa.gov/). STARS codes are available at
797 (https://sites.google.com/view/regime-shift-test/, written in Excel Visual Basic (VBA), R and

MATLAB languages. Python codes used in this study were created and tested based on VBA codes and are available from (will be assigned upon acceptance).

## Declaration of competing interest

The authors declare that they have no known competing financial interests or personal relationships that could have appeared to influence the work reported in this paper.

## Contributions

**Nikolay Nezlin**: Conceptualization, Formal analysis, Methodology, Software, Visualization, Writing – original draft, Writing – review & editing. **SeungHyun Son**: Conceptualization, Data curation, Writing – review & editing. **Christopher Brown**: Conceptualization, Methodology, Writing – review & editing. **Prasanjit Dash**: Conceptualization, Methodology, Writing – review & editing. **Caren Binding**: Conceptualization, Writing – review & editing. **Ashley Elgin**: Writing – review & editing. **Andrea VanderWoude**: Conceptualization, Writing – review & editing.

## Acknowledgments

The authors acknowledge the European Space Agency's efforts to provide the high-quality, open-access OC-CCI dataset. We thank the Ocean Biology Processing Group at NASA Goddard Space Flight Center for single-mission (SeaWiFS, MERIS and MODIS-Aqua) satellite data. Parts of this work were performed and funded under ST13301CQ0050/1332KP22FNEED0042 and the NOAA grant NA24NESX432C0001 (Cooperative Institute for Satellite Earth System Studies - CISESS) at the University of Maryland/ESSIC. This is NOAA GLERL Contribution No. (will be assigned upon acceptance). The comments of two anonymous reviewers were thoughtful and greatly improved the final manuscript. The scientific results and conclusions, as well as any

views or opinions expressed herein, are those of the authors and do not necessarily reflect those of NOAA or the US Department of Commerce.

## References


Adams, H., Ye, J., Persaud, B. D., Slowinski, S., Kheyrollah Pour, H., & Van Cappellen, P. (2022). Rates and timing of chlorophyll-a increases and related environmental variables in global temperate and cold-temperate lakes. Earth Syst. Science Data, 14(11), 5139-5156. https://doi.org/10.5194/essd-14-5139-2022

Allinger, L., & Reavie, E. (2013). The ecological history of Lake Erie as recorded by the phytoplankton community. J. of Great Lakes Res., 39, 365–382. https://doi.org/10.1016/j.jglr.2013.06.014

Antoine, D., Morel, A., Gordon, H. R., Banzon, V. F., & Evans, R. H. (2005). Bridging ocean color observations of the 1980s and 2000s in search of long-term trends. J. of Geophysical Res.: Oceans, 110(C6). https://doi.org/10.1029/2004JC002620

Assel, R. A., Janowiak, J. E., Boyce, D., O'Connors, C., Quinn, F. H., & Norton, D. C. (2000). Laurentian Great Lakes Ice and Weather Conditions for the 1998 El Niño Winter. Bulletin of the American Meteorological Society, 81(4), 703-718. https://doi.org/10.1175/1520-0477(2000)081<0703:LGLIAW>2.3.CO;2

Austin, J., & Colman, S. (2008). A century of temperature variability in Lake Superior. Limnology and Oceanography, 53(6), 2724-2730. https://doi.org/10.4319/lo.2008.53.6.2724

Baldwin, B. S., Mayer, M. S., Dayton, J., Pau, N., Mendilla, J., Sullivan, M., Moore, A., Ma, A., & Mills, E. L. (2002). Comparative growth and feeding in zebra and quagga mussels (*Dreissena polymorpha* and *Dreissena bugensis*): implications for North American lakes. Canadian J. of Fisheries and Aquatic Sciences, 59(4), 680-694. https://doi.org/10.1139/f02-043

Barbiero, R., Lesht, B., & Warren, G. (2011). Evidence for bottom–up control of recent shifts in the pelagic food web of Lake Huron. J. of Great Lakes Res., 37(1), 78-85. https://doi.org/10.1016/j.jglr.2010.11.013

850 Barbiero, R. P., Lesht, B. M., & Warren, G. J. (2012). Convergence of trophic state and the lower
851 food web in Lakes Huron, Michigan and Superior. J. of Great Lakes Res., 38(2), 368-380.
852 https://doi.org/10.1016/j.jglr.2012.03.009
853 Barbiero, R. P., & Tuchman, M. L. (2004). The Deep Chlorophyll Maximum in Lake Superior. J. of
854 Great Lakes Res., 30, 256-268. https://doi.org/10.1016/S0380-1330(04)70390-1
855 Behrenfeld, M. J., O'Malley, R. T., Siegel, D. A., McClain, C. R., Sarmiento, J. L., Feldman, G. C.,
856 Milligan, A. J., Falkowski, P. G., Letelier, R. M., & Boss, E. S. (2006). Climate-driven trends
857 in contemporary ocean productivity. Nature, 444(7120), 752-755.
858 https://doi.org/10.1038/nature05317
859 Benson, A. J. (2014). Chronological History of Zebra and Quagga Mussels (*Dreissenidae*) in North
860 America, 1988–2010. In T. F. Nalepa & D. W. Schloesser (Eds.), Quagga and zebra
861 mussels: biology, impacts, and control (pp. 9–32). CRC Press.
862 https://pubs.usgs.gov/publication/70059274
863 Bergmann, T., Fahnenstiel, G., Lohrenz, S., Millie, D., & Schofield, O. (2004). Impacts of a
864 recurrent resuspension event and variable phytoplankton community composition on
865 remote sensing reflectance. J. of Geophysical Res.: Oceans, 109(C10).
866 https://doi.org/budd10.1029/2002JC001575
867 Binding, C. E., Greenberg, T. A., & Bukata, R. P. (2012). An analysis of MODIS-derived algal and
868 mineral turbidity in Lake Erie. J. of Great Lakes Res., 38(1), 107-116.
869 https://doi.org/10.1016/j.jglr.2011.12.003
870 Binding, C. E., Greenberg, T. A., Bukata, R. P., Smith, D. E., & Twiss, M. R. (2012). The MERIS MCI
871 and its potential for satellite detection of winter diatom blooms on partially ice-covered
872 Lake Erie. J. of Plankton Res., 34(6), 569-573. https://doi.org/10.1093/plankt/fbs021
873 Binding, C. E., Greenberg, T. A., Watson, S. B., Rastin, S., & Gould, J. (2015). Long term water
874 clarity changes in North America's Great Lakes from multi-sensor satellite observations.
875 Limnology and Oceanography, 60(6), 1976-1995. https://doi.org/10.1002/lno.10146
876 Binding, C. E., Zastepa, A., & Zeng, C. (2019). The impact of phytoplankton community
877 composition on optical properties and satellite observations of the 2017 western Lake

878 Erie algal bloom. J. of Great Lakes Res., 45(3), 573-586.
879 https://doi.org/10.1016/j.jglr.2018.11.015
880 Bojinski, S., Verstraete, M., Peterson, T. C., Richter, C., Simmons, A., & Zemp, M. (2014). The
881 Concept of Essential Climate Variables in Support of Climate Research, Applications, and
882 Policy. Bull. of the American Meteorological Society, 95(9), 1431-1443.
883 https://doi.org/10.1175/BAMS-D-13-00047.1
884 Budd, J. W., Drummer, T. D., Nalepa, T. F., & Fahnenstiel, G. L. (2001). Remote sensing of biotic
885 effects: Zebra mussels (*Dreissena polymorpha*) influence on water clarity in Saginaw
886 Bay, Lake Huron. Limnology and Oceanography, 46(2), 213-223.
887 https://doi.org/10.4319/lo.2001.46.2.0213
888 Budd, J. W., & Warrington, D. S. (2004). Satellite-based Sediment and Chlorophyll a Estimates
889 for Lake Superior. J. of Great Lakes Res., 30, 459-466. https://doi.org/10.1016/S0380-
890 1330(04)70406-2
891 Bunnell, D. B., Barbiero, R. P., Ludsin, S. A., Madenjian, C. P., Warren, G. J., Dolan, D. M.,
892 Brenden, T. O., Briland, R., Gorman, O. T., He, J. X., Johengen, T. H., Lantry, B. F., Lesht,
893 B. M., Nalepa, T. F., Riley, S. C., Riseng, C. M., Treska, T. J., Tsehaye, I., WALSH, M. G., . . .
894 Weidel, B. C. (2014). Changing Ecosystem Dynamics in the Laurentian Great Lakes:
895 Bottom-Up and Top-Down Regulation. BioScience, 64(1), 26-39.
896 https://doi.org/10.1093/biosci/bit001
897 Calamita, E., Lever, J. J., Albergel, C., Woolway, R. I., & Odermatt, D. (2024). Detecting climate-
898 related shifts in lakes: A review of the use of satellite Earth Observation. Limnology and
899 Oceanography, 69(4), 723-741. https://doi.org/10.1002/lno.12498
900 Calamita, E., Piccolroaz, S., Majone, B., & Toffolon, M. (2021). On the role of local depth and
901 latitude on surface warming heterogeneity in the Laurentian Great Lakes. Inland Waters,
902 11(2), 208-222. https://doi.org/10.1080/20442041.2021.1873698
903 Campbell, J. W. (1995). The lognormal distribution as a model for bio-optical variability in the
904 sea. J. of Geophysical Res.: Oceans, 100(C7), 13237-13254.
905 https://doi.org/10.1029/95JC00458

Cao, C., Luccia, F. J. D., Xiong, X., Wolfe, R., & Weng, F. (2014). Early On-Orbit Performance of the Visible Infrared Imaging Radiometer Suite Onboard the Suomi National Polar-Orbiting Partnership (S-NPP) Satellite. IEEE Transactions on Geoscience and Remote Sens., 52(2), 1142-1156. https://doi.org/10.1109/TGRS.2013.2247768

Cao, C., Xiong, J., Blonski, S., Liu, Q., Uprety, S., Shao, X., Bai, Y., & Weng, F. (2013). Suomi NPP VIIRS sensor data record verification, validation, and long-term performance monitoring. J. of Geophysical Res.: Atmospheres, 118(20), 11,664-611,678. https://doi.org/10.1002/2013JD020418

Carlton, J. T. (2008). The Zebra Mussel *Dreissena polymorpha* found in North America in 1986 and 1987. J. of Great Lakes Res., 34(4), 770-773. https://doi.org/10.1016/S0380-1330(08)71617-4

Chavez, F. P., Messié, M., & Pennington, J. T. (2011). Marine Primary Production in Relation to Climate Variability and Change. Annual Rev. of Marine Science, 3(1), 227-260. https://doi.org/10.1146/annurev.marine.010908.163917

Claxton, W. T., & Mackie, G. L. (1998). Seasonal and depth variations in gametogenesis and spawning of *Dreissena polymorpha* and *Dreissena bugensis* in eastern Lake Erie. Canadian J. of Zoology, 76(11), 2010-2019. https://doi.org/10.1139/z98-150

Cleveland, R. B., Cleveland, W. S., McRae, J. E., & Terpenning, I. (1990). STL: A seasonal-trend decomposition procedure based on loess. J. of Official Statistics, 6(1), 3-73.

Colebrook, J. M. (1979). Continuous Plankton Records: Seasonal cycles of phytoplankton and copepods in the North Atlantic ocean and the North Sea. Marine Biology, 51(1), 23-32. https://doi.org/10.1007/BF00389027

Conversi, A., Fonda Umani, S., Peluso, T., Molinero, J. C., Santojanni, A., & Edwards, M. (2010). The Mediterranean Sea Regime Shift at the End of the 1980s, and Intriguing Parallelisms with Other European Basins. PLOS ONE, 5(5), e10633. https://doi.org/10.1371/journal.pone.0010633

Diggins, T. P. (2001). A Seasonal Comparison of Suspended Sediment Filtration by Quagga (*Dreissena bugensis*) and Zebra (*D. polymorpha*) Mussels. J. of Great Lakes Res., 27(4), 457-466. https://doi.org/10.1016/S0380-1330(01)70660-0

Donlon, C., Berruti, B., Buongiorno, A., Ferreira, M. H., Féménias, P., Frerick, J., Goryl, P., Klein, U., Laur, H., Mavrocordatos, C., Nieke, J., Rebhan, H., Seitz, B., Stroede, J., & Sciarra, R. (2012). The Global Monitoring for Environment and Security (GMES) Sentinel-3 mission. Remote Sens. of Environ., 120, 37-57. https://doi.org/10.1016/j.rse.2011.07.024

Dove, A., & Chapra, S. C. (2015). Long-term trends of nutrients and trophic response variables for the Great Lakes. Limnology and Oceanography, 60(2), 696-721. https://doi.org/10.1002/lno.10055

Edwards, M., & Richardson, A. J. (2004). Impact of climate change on marine pelagic phenology and trophic mismatch. Nature, 430(7002), 881-884. https://doi.org/10.1038/nature02808

Elgin, A. K., Burlakova, L. E., & Karatayev, A. Y. (2022). Sub-Indicator: Dreissenid Mussels (State of the Great Lakes 2022 Issue. https://binational.net/wp-content/uploads/2023/11/State-of-the-Great-Lakes-2022-%E2%80%93-Technical-Report.pdf

Elgin, A. K., Glyshaw, P. W., & Weidel, B. C. (2022). Depth drives growth dynamics of dreissenid mussels in Lake Ontario. J. of Great Lakes Res., 48(2), 289-299. https://doi.org/10.1016/j.jglr.2021.08.006

Esaias, W. E., Abbott, M. R., Barton, I., Brown, O. B., Campbell, J. W., Carder, K. L., Clark, D. K., Evans, R. H., Hoge, F. E., Gordon, H. R., Balch, W. M., Letelier, R., & Minnett, P. J. (1998). An overview of MODIS capabilities for ocean science observations. IEEE Transactions on Geoscience and Remote Sens., 36(4), 1250-1265. https://doi.org/10.1109/36.701076

Espinoza, I. G., Franco-Gaviria, F., Castañeda, I., Robinson, C., Room, A., Berrío, J. C., Armenteras, D., & Urrego, D. H. (2022). Holocene Fires and Ecological Novelty in the High Colombian Cordillera Oriental [Original Research]. Frontiers in Ecology and Evolution, 10. https://doi.org/10.3389/fevo.2022.895152

European Space Agency. (2022). Ocean Colour Climate Change Initiative dataset, Version 6.0 Product User Guide (D4.2). 6.1). P. M. L. (PML). http://www.esa-oceancolour-cci.org/

962 Evans, M. A., Fahnenstiel, G., & Scavia, D. (2011). Incidental Oligotrophication of North
963 American Great Lakes. Environmental Science & Technology, 45(8), 3297-3303.
964 https://doi.org/10.1021/es103892w
965 Fahnenstiel, G., Pothoven, S., Vanderploeg, H., Klarer, D., Nalepa, T., & Scavia, D. (2010). Recent
966 changes in primary production and phytoplankton in the offshore region of
967 southeastern Lake Michigan. J. of Great Lakes Res., 36, 20-29.
968 https://doi.org/10.1016/j.jglr.2010.03.009
969 Fahnenstiel, G. L., Sayers, M. J., Shuchman, R. A., Yousef, F., & Pothoven, S. A. (2016). Lake-wide
970 phytoplankton production and abundance in the Upper Great Lakes: 2010–2013. J. of
971 Great Lakes Res., 42(3), 619-629. https://doi.org/10.1016/j.jglr.2016.02.004
972 Fahnenstiel, G. L., & Scavia, D. (1987). Dynamics of Lake Michigan Phytoplankton: the Deep
973 Chlorophyll Layer. J. of Great Lakes Res., 13(3), 285-295. https://doi.org/10.1016/S0380-
974 1330(87)71652-9
975 Fichot, C. G., Matsumoto, K., Holt, B., Gierach, M. M., & Tokos, K. S. (2019). Assessing change in
976 the overturning behavior of the Laurentian Great Lakes using remotely sensed lake
977 surface water temperatures. Remote Sens. of Environ., 235, 111427.
978 https://doi.org/https://doi.org/10.1016/j.rse.2019.111427
979 Fraker, M. E., Shrestha, A., Marshall, L., Mason, L., & Miller, R. (2021). Seasonal variation in light
980 penetration and subsurface chlorophyll-α in southern Lake Michigan observed by a
981 glider. J. of Great Lakes Res., 47(4), 1228-1234.
982 https://doi.org/10.1016/j.jglr.2021.04.007
983 Garnesson, P., Mangin, A., Fanton d'Andon, O., Demaria, J., & Bretagnon, M. (2019). The
984 CMEMS GlobColour chlorophyll a product based on satellite observation: multi-sensor
985 merging and flagging strategies. Ocean Science, 15(3), 819-830.
986 https://doi.org/10.5194/os-15-819-2019
987 GCOS. (2011). Systematic Observation Requirements for Satellite-based Products for Climate.
988 2011 update. https://library.wmo.int/idurl/4/48411
989 Glyshaw, P. W., Riseng, C. M., Nalepa, T. F., & Pothoven, S. A. (2015). Temporal trends in
990 condition and reproduction of quagga mussels (*Dreissena rostriformis bugensis*) in

991 southern Lake Michigan. J. of Great Lakes Res., 41, 16-26.
992 https://doi.org/10.1016/j.jglr.2015.08.006
993 Greene, C. H., Meyer-Gutbrod, E., Monger, B. C., McGarry, L. P., Pershing, A. J., Belkin, I. M.,
994 Fratantoni, P. S., Mountain, D. G., Pickart, R. S., Proshutinsky, A., Ji, R., Bisagni, J. J.,
995 Hakkinen, S. M. A., Haidvogel, D. B., Wang, J., Head, E., Smith, P., Reid, P. C., & Conversi,
996 A. (2013). Remote climate forcing of decadal-scale regime shifts in Northwest Atlantic
997 shelf ecosystems. Limnology and Oceanography, 58(3), 803-816.
998 https://doi.org/10.4319/lo.2013.58.3.0803
999 Gregg, W. W., Conkright, M. E., Ginoux, P., O'Reilly, J. E., & Casey, N. W. (2003). Ocean primary
1000 production and climate: Global decadal changes. Geophysical Res. Letters, 30(15), 1809.
1001 https://doi.org/10.1029/2003GL016889
1002 Griffiths, R. W., Schloesser, D. W., Leach, J. H., & Kovalak, W. P. (1991). Distribution and
1003 Dispersal of the Zebra Mussel (*Dreissena polymorpha*) in the Great Lakes Region.
1004 Canadian J. of Fisheries and Aquatic Sciences, 48(8), 1381-1388.
1005 https://doi.org/10.1139/f91-165
1006 Grigorovich, I. A., Kelly, J. R., Darling, J. A., & West, C. W. (2008). The Quagga Mussel Invades
1007 the Lake Superior Basin. J. of Great Lakes Res., 34(2), 342-350.
1008 https://doi.org/10.3394/0380-1330(2008)34[342:TQMITL]2.0.CO;2
1009 Grigorovich, I. A., Korniushin, A. V., Gray, D. K., Duggan, I. C., Colautti, R. I., & MacIsaac, H. J.
1010 (2003). Lake Superior: an invasion coldspot? Hydrobiologia, 499(1), 191-210.
1011 https://doi.org/10.1023/A:1026335300403
1012 Gronewold, A. D., Anderson, E. J., Lofgren, B., Blanken, P. D., Wang, J., Smith, J., Hunter, T.,
1013 Lang, G., Stow, C. A., Beletsky, D., & Bratton, J. (2015). Impacts of extreme 2013–2014
1014 winter conditions on Lake Michigan's fall heat content, surface temperature, and
1015 evaporation. Geophysical Res. Letters, 42(9), 3364-3370.
1016 https://doi.org/10.1002/2015GL063799
1017 Hammond, M. L., Beaulieu, C., Henson, S. A., & Sahu, S. K. (2018). Assessing the Presence of
1018 Discontinuities in the Ocean Color Satellite Record and Their Effects on Chlorophyll

Trends and Their Uncertainties. Geophysical Res. Letters, 45(15), 7654-7662. https://doi.org/10.1029/2017GL076928

Hebert, P. D. N., Muncaster, B. W., & Mackie, G. L. (1989). Ecological and genetic Studies on *Dreissena polymorpha* (Pallas): a new mollusc in the Great Lakes. Canadian J. of Fisheries and Aquatic Sciences, 46(9), 1587-1591. https://doi.org/10.1139/f89-202

Hecky, R. E., Smith, R. E. H., Barton, D. R., Guildford, S. J., Taylor, W. D., Charlton, M. N., & Howell, T. (2004). The nearshore phosphorus shunt: a consequence of ecosystem engineering by dreissenids in the Laurentian Great Lakes. Canadian J. of Fisheries and Aquatic Sciences, 61(7), 1285-1293. https://doi.org/10.1139/f04-065

Henson, S. A., Beaulieu, C., & Lampitt, R. (2016). Observing climate change trends in ocean biogeochemistry: when and where. Glob. Change Biology, 22(4), 1561-1571. https://doi.org/10.1111/gcb.13152

Henson, S. A., Sarmiento, J. L., Dunne, J. P., Bopp, L., Lima, I., Doney, S. C., John, J., & Beaulieu, C. (2010). Detection of anthropogenic climate change in satellite records of ocean chlorophyll and productivity. Biogeosciences, 7(2), 621-640. https://doi.org/10.5194/bg-7-621-2010

Hincks, S. S., & Mackie, G. L. (1997). Effects of pH, calcium, alkalinity, hardness, and chlorophyll on the survival, growth, and reproductive success of zebra mussel (*Dreissena polymorpha*) in Ontario lakes. Canadian J. of Fisheries and Aquatic Sciences, 54(9), 2049-2057. https://doi.org/10.1139/f97-114

Holland, R. E. (1993). Changes in Planktonic Diatoms and Water Transparency in Hatchery Bay, Bass Island Area, Western Lake Erie Since the Establishment of the Zebra Mussel. J. of Great Lakes Res., 19, 617-624. https://doi.org/10.1016/s0380-1330(93)71245-9

Horgan, M. J., & Mills, E. L. (1997). Clearance rates and filtering activity of zebra mussel (*Dreissena polymorpha*): implications for freshwater lakes. Canadian J. of Fisheries and Aquatic Sciences, 54(2), 249-255. https://doi.org/10.1139/f96-276

Hovis, W. A., Clark, D. K., Anderson, F., Austin, R. W., Wilson, W. H., Baker, E. T., Ball, D., Gordon, H. R., Mueller, J. L., El-Sayed, S. Z., Sturm, B., Wrigley, R. C., & Yentsch, C. S.

(1980). Nimbus-7 Coastal Zone Color Scanner: System Description and Initial Imagery. Science, 210(4465), 60-63. https://doi.org/10.1126/science.210.4465.60

Hu, C., Feng, L., Lee, Z., Franz, B. A., Bailey, S. W., Werdell, P. J., & Proctor, C. W. (2019). Improving Satellite Global Chlorophyll a Data Products Through Algorithm Refinement and Data Recovery. J. of Geophysical Res.: Oceans, 124(3), 1524-1543. https://doi.org/10.1029/2019JC014941

International Joint Commission. (1972). Report on Great Lakes Water Quality for 1972. http://www.ijc.org/files/publications/ID610.pdf

IOCCG. (2008). Why Ocean Colour? The Societal Benefits of Ocean-Colour Technology (Reports of the International Ocean-Colour Coordinating Group, Issue. https://repository.oceanbestpractices.org/handle/11329/517

Jackson, T., Sathyendranath, S., & Mélin, F. (2017). An improved optical classification scheme for the Ocean Colour Essential Climate Variable and its applications. Remote Sens. of Environ., 203, 152-161. https://doi.org/10.1016/j.rse.2017.03.036

Johengen, T. H., Biddanda, B. A., & Cotner, J. B. (2008). Stimulation of Lake Michigan Plankton Metabolism by Sediment Resuspension and River Runoff. J. of Great Lakes Res., 34(2), 213-227. https://doi.org/10.3394/0380-1330(2008)34[213:SOLMPM]2.0.CO;2

Karatayev, A., Karatayev, V., Burlakova, L., Mehler, K., Rowe, M., Elgin, A., & Nalepa, T. (2021). Lake morphometry determines *Dreissena* invasion dynamics. Biological Invasions, 23, 2489–2514. https://doi.org/10.1007/s10530-021-02518-3

Karatayev, A. Y., & Burlakova, L. E. (2022). *Dreissena* in the Great Lakes: what have we learned in 30 years of invasion. Hydrobiologia. https://doi.org/10.1007/s10750-022-04990-x

Karatayev, A. Y., Burlakova, L. E., Mehler, K., Barbiero, R. P., Hinchey, E. K., Collingsworth, P. D., Kovalenko, K. E., & Warren, G. (2018). Life after *Dreissena*: The decline of exotic suspension feeder may have significant impacts on lake ecosystems. J. of Great Lakes Res., 44(4), 650-659. https://doi.org/10.1016/j.jglr.2018.05.010

Karatayev, A. Y., Burlakova, L. E., Mehler, K., Bocaniov, S. A., Collingsworth, P. D., Warren, G., Kraus, R. T., & Hinchey, E. K. (2018). Biomonitoring using invasive species in a large Lake:

*Dreissena* distribution maps hypoxic zones. J. of Great Lakes Res., 44(4), 639-649. https://doi.org/10.1016/j.jglr.2017.08.001

Karatayev, A. Y., Burlakova, L. E., Mehler, K., Elgin, A. K., Rudstam, L. G., Watkins, J. M., & Wick, M. (2022). *Dreissena* in Lake Ontario 30 years post-invasion. J. of Great Lakes Res., 48(2), 264-273. https://doi.org/10.1016/j.jglr.2020.11.010

Karatayev, A. Y., Burlakova, L. E., & Padilla, D. K. (2015). Zebra versus quagga mussels: a review of their spread, population dynamics, and ecosystem impacts. Hydrobiologia, 746(1), 97-112. https://doi.org/10.1007/s10750-014-1901-x

Karatayev, A. Y., Karatayev, V. A., Burlakova, L. E., Rowe, M. D., Mehler, K., & Clapsadl, M. D. (2018). Food depletion regulates the demography of invasive dreissenid mussels in a stratified lake. Limnology and Oceanography, 63(5), 2065-2079. https://doi.org/10.1002/lno.10924

Kayastha, M. B., Huang, C., Wang, J., Pringle, W. J., Chakraborty, T., Yang, Z., Hetland, R. D., Qian, Y., & Xue, P. (2023). Insights on Simulating Summer Warming of the Great Lakes: Understanding the Behavior of a Newly Developed Coupled Lake-Atmosphere Modeling System. J. of Advances in Modeling Earth Systems, 15(7), e2023MS003620. https://doi.org/10.1029/2023MS003620

Kerfoot, W. C., Yousef, F., Green, S. A., Budd, J. W., Schwab, D. J., & Vanderploeg, H. A. (2010). Approaching storm: Disappearing winter bloom in Lake Michigan. J. of Great Lakes Res., 36, 30-41. https://doi.org/10.1016/j.jglr.2010.04.010

Kovalenko, K. E., Reavie, E. D., Barbiero, R. P., Burlakova, L. E., Karatayev, A. Y., Rudstam, L. G., & Watkins, J. M. (2018). Patterns of long-term dynamics of aquatic communities and water quality parameters in the Great Lakes: Are they synchronized? J. of Great Lakes Res., 44(4), 660-669. https://doi.org/10.1016/j.jglr.2018.05.018

Kryger, J., & Riisgård, H. U. (1988). Filtration rate capacities in 6 species of European freshwater bivalves. Oecologia, 77(1), 34-38. https://doi.org/10.1007/BF00380921

Kumar, A., Wang, W., Hoerling, M. P., Leetmaa, A., & Ji, M. (2001). The Sustained North American Warming of 1997 and 1998. J. of Climate, 14(3), 345-353. https://doi.org/10.1175/1520-0442(2001)014<0345:TSNAWO>2.0.CO;2

Lavender, S., Jackson, T., & Sathyendranath, S. (2015). The Ocean Colour Climate Change Initiative: Merging ocean colour observations seamlessly. Ocean Challenge, 21, 29-31.

Lee, Z., Carder, K. L., & Arnone, R. A. (2002). Deriving inherent optical properties from water color: a multiband quasi-analytical algorithm for optically deep waters. Applied Optics, 41(27), 5755-5772. https://doi.org/10.1364/AO.41.005755

Lesht, B. M., Barbiero, R. P., & Warren, G. J. (2013). A band-ratio algorithm for retrieving open-lake chlorophyll values from satellite observations of the Great Lakes. J. of Great Lakes Res., 39(1), 138-152. https://doi.org/10.1016/j.jglr.2012.12.007

Lin, P., & Guo, L. (2016). Do invasive quagga mussels alter CO2 dynamics in the Laurentian Great Lakes? Scientific Reports, 6(1), 39078. https://doi.org/10.1038/srep39078

Lower, E., Sturtevant, R., Iott, S., Martinez, F., Rutherford, E., Mason, D. M., Redinger, J., & Elgin, A. K. (2024). The Great Lakes' most unwanted: Characterizing the impacts of the top ten Great Lakes aquatic invasive species. J. of Great Lakes Res., 102365. https://doi.org/10.1016/j.jglr.2024.102365

Madenjian, C. P., Bunnell, D. B., Warner, D. M., Pothoven, S. A., Fahnenstiel, G. L., Nalepa, T. F., Vanderploeg, H. A., Tsehaye, I., Claramunt, R. M., & Clark, R. D. (2015). Changes in the Lake Michigan food web following dreissenid mussel invasions: A synthesis. J. of Great Lakes Res., 41, 217-231. https://doi.org/10.1016/j.jglr.2015.08.009

Makarewicz, J. C., Lewis, T. W., & Bertram, P. (1999). Phytoplankton Composition and Biomass in the Offshore Waters of Lake Erie: Pre- and Post- *Dreissena* Introduction (1983-1993). J. of Great Lakes Res., 25, 135-148. https://doi.org/10.1016/s0380-1330(99)70722-7

Malkin, S. Y., Silsbe, G. M., Smith, R. E. H., & Howell, E. T. (2012). A deep chlorophyll maximum nourishes benthic filter feeders in the coastal zone of a large clear lake. Limnology and Oceanography, 57(3), 735-748. https://doi.org/10.4319/lo.2012.57.3.0735

Mantua, N. J., Hare, S. R., Zhang, Y., Wallace, J. M., & Francis, R. C. (1997). A Pacific Interdecadal Climate Oscillation with Impacts on Salmon Production. Bull. of the American Meteorological Society, 78(6), 1069-1080. https://doi.org/10.1175/1520-0477(1997)078<1069:APICOW>2.0.CO;2

Maritorena, S., d'Andon, O. H. F., Mangin, A., & Siegel, D. A. (2010). Merged satellite ocean color data products using a bio-optical model: Characteristics, benefits and issues. Remote Sens. of Environ., 114(8), 1791-1804. https://doi.org/10.1016/j.rse.2010.04.002

Martinez, E., Antoine, D., D'Ortenzio, F., & Gentili, B. (2009). Climate-Driven Basin-Scale Decadal Oscillations of Oceanic Phytoplankton. Science, 326(5957), 1253-1256. https://doi.org/10.1126/science.1177012

Marty, C. (2008). Regime shift of snow days in Switzerland. Geophysical Res. Letters, 35(12), L12501. https://doi.org/10.1029/2008GL033998

McClain, C. R., Feldman, G. C., & Hooker, S. B. (2004). An overview of the SeaWiFS project and strategies for producing a climate research quality global ocean bio-optical time series. Deep Sea Res. Part II: Topical Stud. in Oceanography, 51(1), 5-42. https://doi.org/10.1016/j.dsr2.2003.11.001

McClain, C. R., M.L. Cleave, G.C. Feldman, W.W. Gregg, S.B. Hooker and N. Kuring. (1998). Science quality SeaWiFS data for global biosphere research. Sea Technology, 39, 10-16.

Meis, S., Thackerray, S. J., & Jones, I. D. (2009). Effects of recent climate change on phytoplankton phenology in a temperate lake. Freshw. Biology, 54(9), 1888-1898. https://doi.org/10.1111/j.1365-2427.2009.02240.x

Mélin, F. (2016). Impact of inter-mission differences and drifts on chlorophyll-a trend estimates. International J. of Remote Sens., 37(10), 2233-2251. https://doi.org/10.1080/01431161.2016.1168949

Mélin, F., Vantrepotte, V., Chuprin, A., Grant, M., Jackson, T., & Sathyendranath, S. (2017). Assessing the fitness-for-purpose of satellite multi-mission ocean color climate data records: A protocol applied to OC-CCI chlorophyll-a data. Remote Sens. of Environ., 203, 139-151. https://doi.org/10.1016/j.rse.2017.03.039

Méthot, J., Huang, X., & Grover, H. (2015). Demographics and societal values as drivers of change in the Great Lakes–St. Lawrence River basin. J. of Great Lakes Res., 41, 30-44. https://doi.org/10.1016/j.jglr.2014.11.001

Michalak, A. M., Anderson, E. J., Beletsky, D., Boland, S., Bosch, N. S., Bridgeman, T. B., Chaffin, J. D., Cho, K., Confesor, R., Daloğlu, I., DePinto, J. V., Evans, M. A., Fahnenstiel, G. L., He,

L., Ho, J. C., Jenkins, L., Johengen, T. H., Kuo, K. C., LaPorte, E., . . . Zagorski, M. A. (2013). Record-setting algal bloom in Lake Erie caused by agricultural and meteorological trends consistent with expected future conditions. Proc. of the Natl. Academy of Sciences, 110(16), 6448-6452. https://doi.org/10.1073/pnas.1216006110

Mida, J. L., Scavia, D., Fahnenstiel, G. L., Pothoven, S. A., Vanderploeg, H. A., & Dolan, D. M. (2010). Long-term and recent changes in southern Lake Michigan water quality with implications for present trophic status. J. of Great Lakes Res., 36, 42-49. https://doi.org/10.1016/j.jglr.2010.03.010

Millard, E. S., Myles, D. D., Johannsson, O. E., & Ralph, K. M. (1996). Phytoplankton photosynthesis at two index stations in Lake Ontario 1987-1992: Assessment of the long-term response to phosphorus control. Canadian J. of Fisheries and Aquatic Sciences, 53(5), 1092-1111. https://doi.org/10.1139/f96-029

Möllmann, C., & Diekmann, R. (2012). Chapter 4 - Marine Ecosystem Regime Shifts Induced by Climate and Overfishing: A Review for the Northern Hemisphere. In G. Woodward, U. Jacob, & E. J. O'Gorman (Eds.), Advances in Ecological Res. (Vol. 47, pp. 303-347). Academic Press. https://doi.org/10.1016/B978-0-12-398315-2.00004-1

Möllmann, C., Diekmann, R., Müller-Karulis, B., Kornilovs, G., Plikshs, M., & Axe, P. (2009). Reorganization of a large marine ecosystem due to atmospheric and anthropogenic pressure: a discontinuous regime shift in the Central Baltic Sea. Glob. Change Biology, 15(6), 1377-1393. https://doi.org/10.1111/j.1365-2486.2008.01814.x

Moore, T. S., Mouw, C. B., Sullivan, J. M., Twardowski, M. S., Burtner, A. M., Ciochetto, A. B., McFarland, M. N., Nayak, A. R., Paladino, D., Stockley, N. D., Johengen, T. H., Yu, A. W., Ruberg, S., & Weidemann, A. (2017). Bio-optical Properties of Cyanobacteria Blooms in Western Lake Erie [Original Research]. Frontiers in Marine Science, 4. https://doi.org/10.3389/fmars.2017.00300

Mouw, C. B., Chen, H., McKinley, G. A., Effler, S., O'Donnell, D., Perkins, M. G., & Strait, C. (2013). Evaluation and optimization of bio-optical inversion algorithms for remote sensing of Lake Superior's optical properties. J. of Geophysical Res.: Oceans, 118(4), 1696-1714. https://doi.org/10.1002/jgrc.20139

1190 Mouw, C. B., Ciochetto, A. B., Grunert, B., & Yu, A. (2017). Expanding understanding of optical
1191 variability in Lake Superior with a 4-year dataset. Earth Syst. Sci. Data, 9(2), 497-509.
1192 https://doi.org/10.5194/essd-9-497-2017
1193 Nalepa, T. F., Fanslow, D. L., & Lang, G. A. (2009). Transformation of the offshore benthic
1194 community in Lake Michigan: recent shift from the native amphipod Diporeia spp. to the
1195 invasive mussel *Dreissena rostriformis bugensis*. Freshw. Biology, 54(3), 466-479.
1196 https://doi.org/10.1111/j.1365-2427.2008.02123.x
1197 Nalepa, T. F., Fanslow, D. L., & Pothoven, S. A. (2010). Recent changes in density, biomass,
1198 recruitment, size structure, and nutritional state of *Dreissena* populations in southern
1199 Lake Michigan. J. of Great Lakes Res., 36, 5-19.
1200 https://doi.org/10.1016/j.jglr.2010.03.013
1201 Newman, M., Alexander, M. A., Ault, T. R., Cobb, K. M., Deser, C., Di Lorenzo, E., Mantua, N. J.,
1202 Miller, A. J., Minobe, S., Nakamura, H., Schneider, N., Vimont, D. J., Phillips, A. S., Scott,
1203 J. D., & Smith, C. A. (2016). The Pacific Decadal Oscillation, Revisited. J. of Climate,
1204 29(12), 4399-4427. https://doi.org/10.1175/JCLI-D-15-0508.1
1205 Nicholls, K. H., Hopkins, G. J., & Standke, S. J. (1999). Reduced chlorophyll to phosphorus ratios
1206 in nearshore Great Lakes waters coincide with the establishment of dreissenid mussels.
1207 Canadian J. of Fisheries and Aquatic Sciences, 56(1), 153-161.
1208 https://doi.org/10.1139/f98-149
1209 Nieke, J., Borde, F., Mavrocordatos, C., Berruti, B., Delclaud, Y., Riti, J. B., & Garnier, T. (2012).
1210 The Ocean and Land Colour Imager (OLCI) for the Sentinel 3 GMES Mission: status and
1211 first test results (Vol. 8528). SPIE. https://doi.org/10.1117/12.977247
1212 O'Reilly, C. M., Sharma, S., Gray, D. K., Hampton, S. E., Read, J. S., Rowley, R. J., Schneider, P.,
1213 Lenters, J. D., McIntyre, P. B., Kraemer, B. M., Weyhenmeyer, G. A., Straile, D., Dong, B.,
1214 Adrian, R., Allan, M. G., Anneville, O., Arvola, L., Austin, J., Bailey, J. L., . . . Zhang, G.
1215 (2015). Rapid and highly variable warming of lake surface waters around the globe.
1216 Geophysical Res. Letters, 42(24), 10,773-710,781.
1217 https://doi.org/10.1002/2015GL066235

O'Reilly, J. E., & Werdell, P. J. (2019). Chlorophyll algorithms for ocean color sensors - OC4, OC5 & OC6. Remote Sens. of Environ., 229, 32-47. https://doi.org/10.1016/j.rse.2019.04.021

Padilla, D. K., Adolph, S. C., Cottingham, K. L., & Schneider, D. W. (1996). Predicting the consequences of dreissenid mussels on a pelagic food web. Ecological Modelling, 85(2), 129-144. https://doi.org/10.1016/0304-3800(94)00185-5

Parkinson, C. L. (2003). Aqua: an Earth-Observing Satellite mission to examine water and other climate variables. IEEE Transactions on Geoscience and Remote Sens., 41(2), 173-183. https://doi.org/10.1109/TGRS.2002.808319

Pillsbury, R., Lowe, R., Pan, Y., & Greenwood, J. (2002). Changes in the Benthic Algal Community and Nutrient Limitation in Saginaw Bay, Lake Huron, during the Invasion of the Zebra Mussel (*Dreissena polymorpha*). J. of the North American Benthological Society, 21(2), 238-252. https://doi.org/10.2307/1468412

Pothoven, S. A., & Fahnenstiel, G. L. (2013). Recent change in summer chlorophyll a dynamics of southeastern Lake Michigan. J. of Great Lakes Res., 39(2), 287-294. https://doi.org/10.1016/j.jglr.2013.02.005

Pothoven, S. A., & Fahnenstiel, G. L. (2015). Spatial and temporal trends in zooplankton assemblages along a nearshore to offshore transect in southeastern Lake Michigan from 2007 to 2012. J. of Great Lakes Res., 41, 95-103. https://doi.org/10.1016/j.jglr.2014.09.015

Pothoven, S. A., & Vanderploeg, H. A. (2020). Seasonal patterns for Secchi depth, chlorophyll a, total phosphorus, and nutrient limitation differ between nearshore and offshore in Lake Michigan. J. of Great Lakes Res., 46(3), 519-527. https://doi.org/10.1016/j.jglr.2020.03.013

Quinn, F. H. (1992). Hydraulic Residence Times for the Laurentian Great Lakes. J. of Great Lakes Res., 18(1), 22-28. https://doi.org/10.1016/S0380-1330(92)71271-4

Rast, M., Bezy, J. L., & Bruzzi, S. (1999). The ESA Medium Resolution Imaging Spectrometer MERIS a review of the instrument and its mission. International J. of Remote Sens., 20(9), 1681-1702. https://doi.org/10.1080/014311699212416

1246 Reavie, E. D., Barbiero, R. P., Allinger, L. E., & Warren, G. J. (2014). Phytoplankton trends in the
1247 Great Lakes, 2001–2011. J. of Great Lakes Res., 40(3), 618-639.
1248 https://doi.org/10.1016/j.jglr.2014.04.013
1249 Reid, P. C., Hari, R. E., Beaugrand, G., Livingstone, D. M., Marty, C., Straile, D., Barichivich, J.,
1250 Goberville, E., Adrian, R., Aono, Y., Brown, R., Foster, J., Groisman, P., Hélaouët, P., Hsu,
1251 H.-H., Kirby, R., Knight, J., Kraberg, A., Li, J., . . . Zhu, Z. (2016). Global impacts of the
1252 1980s regime shift. Glob. Change Biology, 22(2), 682-703.
1253 https://doi.org/10.1111/gcb.13106
1254 Ricciardi, A., & MacIsaac, H. J. (2000). Recent mass invasion of the North American Great Lakes
1255 by Ponto-Caspian species. Trends in Ecology & Evolution, 15(2), 62-65.
1256 https://doi.org/10.1016/S0169-5347(99)01745-0
1257 Rodionov, S., & Overland, J. E. (2005). Application of a sequential regime shift detection method
1258 to the Bering Sea ecosystem. ICES J. of Marine Science, 62(3), 328-332.
1259 https://doi.org/10.1016/j.icesjms.2005.01.013
1260 Rodionov, S. N. (2004). A sequential algorithm for testing climate regime shifts. Geophysical
1261 Res. Letters, 31(9), L09204. https://doi.org/10.1029/2004GL019448
1262 Rodionov, S. N. (2006). Use of prewhitening in climate regime shift detection. Geophysical Res.
1263 Letters, 33(12). https://doi.org/10.1029/2006GL025904
1264 Roe, S. L., & MacIsaac, H. J. (1997). Deepwater population structure and reproductive state of
1265 quagga mussels (*Dreissena bugensis*) in Lake Erie. Canadian J. of Fisheries and Aquatic
1266 Sciences, 54(10), 2428-2433. https://doi.org/10.1139/f97-151
1267 Rowe, M. D., Anderson, E. J., Vanderploeg, H. A., Pothoven, S. A., Elgin, A. K., Wang, J., &
1268 Yousef, F. (2017). Influence of invasive quagga mussels, phosphorus loads, and climate
1269 on spatial and temporal patterns of productivity in Lake Michigan: A biophysical
1270 modeling study. Limnology and Oceanography, 62(6), 2629-2649.
1271 https://doi.org/10.1002/lno.10595
1272 Rowe, M. D., Obenour, D. R., Nalepa, T. F., Vanderploeg, H. A., Yousef, F., & Kerfoot, W. C.
1273 (2015). Mapping the spatial distribution of the biomass and filter-feeding effect of

invasive dreissenid mussels on the winter-spring phytoplankton bloom in Lake Michigan. Freshw. Biology, 60(11), 2270-2285. https://doi.org/10.1111/fwb.12653

Sathyendranath, S., Brewin, R. J. W., Brockmann, C., Brotas, V., Calton, B., Chuprin, A., Cipollini, P., Couto, A. B., Dingle, J., Doerffer, R., Donlon, C., Dowell, M., Farman, A., Grant, M., Groom, S., Horseman, A., Jackson, T., Krasemann, H., Lavender, S., . . . Platt, T. (2019). An Ocean-Colour Time Series for Use in Climate Studies: The Experience of the Ocean-Colour Climate Change Initiative (OC-CCI). Sensors, 19(19), 4285. https://doi.org/10.3390/s19194285

Sayers, M., Bosse, K., Fahnenstiel, G., & Shuchman, R. (2020). Carbon Fixation Trends in Eleven of the World's Largest Lakes: 2003–2018. Water, 12(12), 3500. https://doi.org/10.3390/w12123500

Sayers, M. J., Bosse, K. R., Shuchman, R. A., Ruberg, S. A., Fahnenstiel, G. L., Leshkevich, G. A., Stuart, D. G., Johengen, T. H., Burtner, A. M., & Palladino, D. (2019). Spatial and temporal variability of inherent and apparent optical properties in western Lake Erie: Implications for water quality remote sensing. J. of Great Lakes Res., 45(3), 490-507. https://doi.org/10.1016/j.jglr.2019.03.011

Scavia, D., David Allan, J., Arend, K. K., Bartell, S., Beletsky, D., Bosch, N. S., Brandt, S. B., Briland, R. D., Daloğlu, I., DePinto, J. V., Dolan, D. M., Evans, M. A., Farmer, T. M., Goto, D., Han, H., Höök, T. O., Knight, R., Ludsin, S. A., Mason, D., . . . Zhou, Y. (2014). Assessing and addressing the re-eutrophication of Lake Erie: Central basin hypoxia. J. of Great Lakes Res., 40(2), 226-246. https://doi.org/10.1016/j.jglr.2014.02.004

Schelske, C. L., Rothman, E. D., Stoermer, E. F., & Santiago, M. A. (1974). Responses of phosphorus limited Lake Michigan phytoplankton to factorial enrichments with nitrogen and phosphorus1. Limnology and Oceanography, 19(3), 409-419. https://doi.org/10.4319/lo.1974.19.3.0409

Schneider, P., & Hook, S. J. (2010). Space observations of inland water bodies show rapid surface warming since 1985. Geophysical Res. Letters, 37(22). https://doi.org/10.1029/2010GL045059

1302 Scofield, A. E., Watkins, J. M., Osantowski, E., & Rudstam, L. G. (2020). Deep chlorophyll maxima
1303 across a trophic state gradient: A case study in the Laurentian Great Lakes. Limnology
1304 and Oceanography, 65(10), 2460-2484. https://doi.org/10.1002/lno.11464
1305 Shuchman, R. A., Leshkevich, G., Sayers, M. J., Johengen, T. H., Brooks, C. N., & Pozdnyakov, D.
1306 (2013). An algorithm to retrieve chlorophyll, dissolved organic carbon, and suspended
1307 minerals from Great Lakes satellite data. J. of Great Lakes Res., 39, 14-33.
1308 https://doi.org/10.1016/j.jglr.2013.06.017
1309 Siegel, D. A., Doney, S. C., & Yoder, J. A. (2002). The North Atlantic Spring Phytoplankton Bloom
1310 and Sverdrup's Critical Depth Hypothesis. Science, 296(5568), 730-733.
1311 https://doi.org/10.1126/science.1069174
1312 Son, S., & Wang, M. (2019). VIIRS-Derived Water Turbidity in the Great Lakes. Remote Sens.,
1313 11(12), 1448. https://doi.org/10.3390/rs11121448
1314 Son, S., & Wang, M. (2020). Water Quality Properties Derived from VIIRS Measurements in the
1315 Great Lakes. Remote Sens., 12(10), 1605. https://doi.org/10.3390/rs12101605
1316 Sterner, R. W. (2021). The Laurentian Great Lakes: A Biogeochemical Test Bed. Annual Rev. of
1317 Earth and Planet. Sciences, 49, 201-229. https://doi.org/10.1146/annurev-earth-
1318 071420-051746
1319 Sterner, R. W., Ostrom, P., Ostrom, N. E., Klump, J. V., Steinman, A. D., Dreelin, E. A., Vander
1320 Zanden, M. J., & Fisk, A. T. (2017). Grand challenges for research in the Laurentian Great
1321 Lakes. Limnology and Oceanography, 62(6), 2510-2523.
1322 https://doi.org/10.1002/lno.10585
1323 Sterner, R. W., Reinl, K. L., Lafrancois, B. M., Brovold, S., & Miller, T. R. (2020). A first
1324 assessment of cyanobacterial blooms in oligotrophic Lake Superior. Limnology and
1325 Oceanography, 65(12), 2984-2998. https://doi.org/10.1002/lno.11569
1326 Stevens, R. J. J., & Neilson, M. A. (1987). Response of Lake Ontario to Reductions in Phosphorus
1327 Load, 1967–82. Canadian J. of Fisheries and Aquatic Sciences, 44(12), 2059-2068.
1328 https://doi.org/10.1139/f87-255

Stirnimann, L., Conversi, A., & Marini, S. (2019). Detection of regime shifts in the environment: testing “STARS” using synthetic and observed time series. ICES J. of Marine Science, 76(7), 2286-2296. https://doi.org/10.1093/icesjms/fsz148

Stoeckmann, A. (2003). Physiological energetics of Lake Erie dreissenid mussels: a basis for the displacement of *Dreissena polymorpha* by *Dreissena bugensis*. Canadian J. of Fisheries and Aquatic Sciences, 60(2), 126-134. https://doi.org/10.1139/f03-005

Stoermer, E. F., Wolin, J. A., Schelske, C. L., & Conley, D. J. (1990). Siliceous microfossil succession in Lake Michigan. Limnology and Oceanography, 35(4), 959-967. https://doi.org/10.4319/lo.1990.35.4.0959

Strayer, D. L., Adamovich, B. V., Adrian, R., Aldridge, D. C., Balogh, C., Burlakova, L. E., Fried-Petersen, H. B., G.-Tóth, L., Hetherington, A. L., Jones, T. S., Karatayev, A. Y., Madill, J. B., Makarevich, O. A., Marsden, J. E., Martel, A. L., Minchin, D., Nalepa, T. F., Noordhuis, R., Robinson, T. J., . . . Jeschke, J. M. (2019). Long-term population dynamics of dreissenid mussels (*Dreissena polymorpha* and *D. rostriformis*): a cross-system analysis. Ecosphere, 10(4), e02701. https://doi.org/10.1002/ecs2.2701

Stumpf, R. P., Johnson, L. T., Wynne, T. T., & Baker, D. B. (2016). Forecasting annual cyanobacterial bloom biomass to inform management decisions in Lake Erie. J. of Great Lakes Res., 42(6), 1174-1183. https://doi.org/10.1016/j.jglr.2016.08.006

Stumpf, R. P., & Pennock, J. R. (1989). Calibration of a general optical equation for remote sensing of suspended sediments in a moderately turbid estuary. J. of Geophysical Res.: Oceans, 94(C10), 14363-14371. https://doi.org/10.1029/JC094iC10p14363

Stumpf, R. P., & Pennock, J. R. (1991). Remote estimation of the diffuse attenuation coefficient in a moderately turbid estuary. Remote Sens. of Environ., 38(3), 183-191. https://doi.org/10.1016/0034-4257(91)90088-N

Stumpf, R. P., Wynne, T. T., Baker, D. B., & Fahnenstiel, G. L. (2012). Interannual Variability of Cyanobacterial Blooms in Lake Erie. PLOS ONE, 7(8), e42444. https://doi.org/10.1371/journal.pone.0042444

Sverdrup, H. U. (1953). On Conditions for the Vernal Blooming of Phytoplankton. ICES J. of Marine Science, 18(3), 287-295. https://doi.org/10.1093/icesjms/18.3.287

1358 Tian, Y., Kidokoro, H., Watanabe, T., & Iguchi, N. (2008). The late 1980s regime shift in the
1359 ecosystem of Tsushima warm current in the Japan/East Sea: Evidence from historical
1360 data and possible mechanisms. Prog. in Oceanography, 77(2), 127-145.
1361 https://doi.org/10.1016/j.pocean.2008.03.007
1362 Trebitz, A. S., Hatzenbuhler, C. L., Hoffman, J. C., Meredith, C. S., Peterson, G. S., Pilgrim, E. M.,
1363 Barge, J. T., Cotter, A. M., & Wick, M. J. (2019). *Dreissena* veligers in western Lake
1364 Superior – Inference from new low-density detection. J. of Great Lakes Res., 45(3), 691-
1365 699. https://doi.org/10.1016/j.jglr.2019.03.013
1366 Twiss, M. R., McKay, R. M. L., Bourbonniere, R. A., Bullerjahn, G. S., Carrick, H. J., Smith, R. E. H.,
1367 Winter, J. G., D'Souza, N. A., Furey, P. C., Lashaway, A. R., Saxton, M. A., & Wilhelm, S.
1368 W. (2012). Diatoms abound in ice-covered Lake Erie: An investigation of offshore winter
1369 limnology in Lake Erie over the period 2007 to 2010. J. of Great Lakes Res., 38(1), 18-30.
1370 https://doi.org/10.1016/j.jglr.2011.12.008 (rea)
1371 Valente, A., Sathyendranath, S., Brotas, V., Groom, S., Grant, M., Jackson, T., Chuprin, A.,
1372 Taberner, M., Airs, R., Antoine, D., Arnone, R., Balch, W. M., Barker, K., Barlow, R.,
1373 Bélanger, S., Berthon, J. F., Beşiktepe, Ş., Borsheim, Y., Bracher, A., . . . Zibordi, G. (2022).
1374 A compilation of global bio-optical in situ data for ocean colour satellite applications –
1375 version three. Earth Syst. Science Data, 14(12), 5737-5770.
1376 https://doi.org/10.5194/essd-14-5737-2022
1377 Van Cleave, K., Lenters, J. D., Wang, J., & Verhamme, E. M. (2014). A regime shift in Lake
1378 Superior ice cover, evaporation, and water temperature following the warm El Niño
1379 winter of 1997–1998. Limnology and Oceanography, 59(6), 1889-1898.
1380 https://doi.org/10.4319/lo.2014.59.6.1889
1381 Vanderploeg, H. A., Johengen, T. H., Lavrentyev, P. J., Chen, C., Lang, G. A., Agy, M. A., Bundy,
1382 M. H., Cavaletto, J. F., Eadie, B. J., Liebig, J. R., Miller, G. S., Ruberg, S. A., & McCormick,
1383 M. J. (2007). Anatomy of the recurrent coastal sediment plume in Lake Michigan and its
1384 impacts on light climate, nutrients, and plankton. J. of Geophysical Res.: Oceans,
1385 112(C3), C03S90. https://doi.org/10.1029/2004JC002379

Vanderploeg, H. A., Liebig, J. R., Nalepa, T. F., Fahnenstiel, G. L., & Pothoven, S. A. (2010). *Dreissena* and the disappearance of the spring phytoplankton bloom in Lake Michigan. J. of Great Lakes Res., 36, 50-59. https://doi.org/10.1016/j.jglr.2010.04.005

Vantrepotte, V., & Mélin, F. (2009). Temporal variability of 10-year global SeaWiFS time-series of phytoplankton chlorophyll a concentration. ICES J. of Marine Science, 66(7), 1547-1556. https://doi.org/10.1093/icesjms/fsp107

Vollenweider, R. A., Munawar, M., & Stadelmann, P. (1974). A Comparative Review of Phytoplankton and Primary Production in the Laurentian Great Lakes. J. of the Fisheries Res. Board of Canada, 31(5), 739-762. https://doi.org/10.1139/f74-100

Wang, H., & Convertino, M. (2023). Algal bloom ties: Systemic biogeochemical stress and Chlorophyll-a shift forecasting. Ecological Indicators, 154, 110760. https://doi.org/10.1016/j.ecolind.2023.110760

Watkins, J. (2009). Comparison of shipboard and satellite measurements of surface water temperature and chlorophyll a in Lake Ontario. Aquatic Ecosystem Health & Management, 12, 271-280. https://doi.org/10.1080/14634980903136180

Watson, S. B., Miller, C., Arhonditsis, G., Boyer, G. L., Carmichael, W., Charlton, M. N., Confesor, R., Depew, D. C., Höök, T. O., Ludsin, S. A., Matisoff, G., McElmurry, S. P., Murray, M. W., Peter Richards, R., Rao, Y. R., Steffen, M. M., & Wilhelm, S. W. (2016). The re-eutrophication of Lake Erie: Harmful algal blooms and hypoxia. Harmful Algae, 56, 44-66. https://doi.org/10.1016/j.hal.2016.04.010

Woodruff, D. L., Stumpf, R. P., Scope, J. A., & Paerl, H. W. (1999). Remote Estimation of Water Clarity in Optically Complex Estuarine Waters. Remote Sens. of Environ., 68(1), 41-52. https://doi.org/10.1016/S0034-4257(98)00108-4

Wynne, T. T., Mishra, S., Meredith, A., Litaker, R. W., & Stumpf, R. P. (2021). Intercalibration of MERIS, MODIS, and OLCI Satellite Imagers for Construction of Past, Present, and Future Cyanobacterial Biomass Time Series. Remote Sens., 13(12), 2305. https://doi.org/10.3390/rs13122305

Wynne, T. T., & Stumpf, R. P. (2015). Spatial and Temporal Patterns in the Seasonal Distribution of Toxic Cyanobacteria in Western Lake Erie from 2002–2014. Toxins, 7(5), 1649-1663. https://doi.org/10.3390/toxins7051649

Xia, Z., MacIsaac, H. J., Hecky, R. E., Depew, D. C., Haffner, G. D., & Weidman, R. P. (2021). Multiple factors regulate filtration by invasive mussels: Implications for whole-lake ecosystems. Science of The Total Environ., 765, 144435. https://doi.org/10.1016/j.scitotenv.2020.144435

Xu, J., Liu, H., Lin, J., Lyu, H., Dong, X., Li, Y., Guo, H., & Wang, H. (2022). Long-term monitoring particulate composition change in the Great Lakes using MODIS data. Water Res., 222, 118932. https://doi.org/10.1016/j.watres.2022.118932

Yousef, F., Charles Kerfoot, W., Shuchman, R., & Fahnenstiel, G. (2014). Bio-optical properties and primary production of Lake Michigan: Insights from 13-years of SeaWiFS imagery. J. of Great Lakes Res., 40(2), 317-324. https://doi.org/10.1016/j.jglr.2014.02.018

Yousef, F., Shuchman, R., Sayers, M., Fahnenstiel, G., & Henareh, A. (2017). Water clarity of the Upper Great Lakes: Tracking changes between 1998–2012. J. of Great Lakes Res., 43(2), 239-247. https://doi.org/10.1016/j.jglr.2016.12.002

Yu, S., Bai, Y., He, X., Gong, F., & Li, T. (2023). A new merged dataset of global ocean chlorophyll-a concentration for better trend detection [Original Research]. Frontiers in Marine Science, 10. https://doi.org/10.3389/fmars.2023.1051619

Yuan, F., Krebs, R. A., & Wagner, A. N. (2021). Identifying the influence of zebra and quagga mussels on sedimentary phosphorus dynamics in western Lake Erie. Hydrobiologia, 848(8), 1897-1909. https://doi.org/10.1007/s10750-021-04565-2

Zhang, Y., Wallace, J. M., & Battisti, D. S. (1997). ENSO-like Interdecadal Variability: 1900–93. J. of Climate, 10(5), 1004-1020. https://doi.org/10.1175/1520-0442(1997)010<1004:ELIV>2.0.CO;2

Zhong, Y., Notaro, M., Vavrus, S. J., & Foster, M. J. (2016). Recent accelerated warming of the Laurentian Great Lakes: Physical drivers. Limnology and Oceanography, 61(5), 1762-1786. https://doi.org/10.1002/lno.10331

Zhou, Y., Obenour, D. R., Scavia, D., Johengen, T. H., & Michalak, A. M. (2013). Spatial and Temporal Trends in Lake Erie Hypoxia, 1987–2007. Environmental Science & Technology, 47(2), 899-905. https://doi.org/10.1021/es303401b

**Table 1. Sensor data used in the construction of the Ocean Colour Climate Change Initiative (OC-CCI) Version 6.0 dataset.**

| Sensor | Satellite | Agency | Data Used in OC-CCI v.6.0 | References |
|---|---|---|---|---|
| SeaWiFS[a] | SeaWiFS[a] | NASA[b] | 1997-2010 | (McClain et al., 2004; McClain, 1998) |
| MODIS[c] | Aqua | NASA[b] | 2002-2019 | (Esaias et al., 1998; Parkinson, 2003) |
| MERIS[d] | Envisat | ESA[e] | 2002-2012 | (Rast et al., 1999) |
| VIIRS[f] | SNPP[g] | NASA[b] | 2012-2019 | (Cao et al., 2014, 2013) |
| OLCI-A[h] | Sentinel-3A | ESA[e] | 2016-2022 | (Donlon et al., 2012; Nieke et al., 2012) |
| OLCI-B[h] | Sentinel-3B | ESA | 2018-2022 | (Donlon et al., 2012; Nieke et al., 2012) |

[a] Sea-viewing Wide-Field-of-view Sensor

[b] National Aeronautics and Space Administration

[c] MODerate-resolution Imaging Spectroradiometer

[d] MEdium spectral Resolution Imaging Spectrometer

[e] European Space Agency

[f] Visible and Infrared Imaging Radiometer Suite

[g] SUOMI National Polar-Orbiting Partnership

[h] Ocean and Land Colour Instrument

**Figure Captions**

**Figure 1.** Bathymetric maps of the Laurentian Great Lakes: (S) Superior, (M) Michigan, (H) Huron, (E) Erie, and (O) Ontario. Depth/elevation grids from https://www.ngdc.noaa.gov /mgg/greatlakes/. White triangle in (M) indicates the center (the location with maximum distance offshore) of Lake Michigan used later in Figures 2 and 3.

**Figure 2.** An example of using (a) the time series of chlorophyll concentration (*Chl-a*; μg $L^{-1}$) in the center of Lake Michigan (latitude 43.047; longitude -87.070; depth 81 m; white triangle in Figure 1M) to determine the Seasonal-Trend decomposition using LOESS (STL). The *Chl-a* time series is split into the (b) seasonal factor (μg $L^{-1}$) and (c) smoothed trend (blue line; μg $L^{-1}$) and residuals (black line; μg $L^{-1}$). Regime shifts (solid red lines in (c)) are detected in the "deseasonalized" time series (the sum of trend and residuals) using the Sequential T-test Analysis of Regime Shifts (STARS) method.

**Figure 3.** (a)—Monthly median chlorophyll concentrations (dots) and its five-year median (filled triangles) in the center of southern Lake Michigan (white triangle in Figure 1M) for the 'starting' (1998-2002; blue line; upward pointing triangles) and 'ending' (2018-2022; red line; downward pointing triangles) five-year periods of OC-CCI observations. (b)—Median monthly mean chlorophyll concentrations (blue polygon 1998-2002; red polygon 2018-2022) and the timings of annual maxima (arrows pointing through the centers of gravity represented by blue and red stars to the external circle representing a 12-month cycle) plotted in polar coordinates. The magnitude of average monthly median *Chl-a* is represented as the distance from the center of polar coordinates. In both 3a and 3b, the values of 3.5 and 10.8, indicate the timings in months of *Chl-a* maximum during 1998-2002 and 2018-2022, respectively.

**Figure 4.** Trends and regime shifts detected by the integrated STL-STARS method in median chlorophyll concentration (*Chl-a*) of (a, c, e, g) Lake Michigan and (b, d, f, h) Lake Huron based on observations of (a-b) OC-CCI, (c-d) SeaWiFS, (e-f) MODIS-Aqua, and (g-h) MERIS. Red circular markers indicate outliers, i.e., the values exceeding two standard deviations. Red dotted vertical lines indicate regime shifts; red horizontal lines indicate regime means.

**Figure 5.** Trends and regime shifts detected by the integrated STL-STARS method in OC-CCI median chlorophyll concentration (*Chl-a*) in Lakes (S) Superior, (M) Michigan, (H) Huron, (E) Erie and (O) Ontario. Red circular markers indicate outliers, i.e., the values exceeding two standard deviations. Red dotted vertical lines indicate regime shifts; red numbers indicate the years of regime shifts; red horizontal lines indicate regime means.

**Figure 6.** Maps of the year in which chlorophyll concentrations (*Chl-a*) stabilized at a lower level in Lakes (S) Superior, (M) Michigan, (H) Huron, (E) Erie and (O) Ontario. White color indicates that no significant decrease in *Chl-a* was detected during the period (1997-2022) examined.

**Figure 7.** Maps of the difference (in percent) of chlorophyll concentration (*Chl-a*) between the 'initial' (starting 1997) and 'final' (see Figure 6) regimes in Lakes (S) Superior, (M) Michigan, (H) Huron, (E) Erie and (O) Ontario. White color indicates that no significant decrease in *Chl-a* was detected during the period examined.

**Figure 8.** Difference (in percent) of chlorophyll concentration (*Chl-a*) between the 'initial' and 'final' regimes (Figure 7) in relation to bathymetry in Lakes (S) Superior, (M) Michigan, (H) Huron, (E) Erie and (O) Ontario. The magnitudes of *Chl-a* decrease in 12-km grid cells (circles) were smoothed with LOESS function (black lines).

**Figure 9.** Seasonal cycles of monthly median chlorophyll concentrations (*Chl-a*) in the 'starting' (1998-2002; blue line; upward pointing triangles) and 'ending' (2018-2022; red line; downward pointing triangles) five-year periods of the Ocean Colour Climate Change Initiative (OC-CCI) dataset in Lakes (S) Superior, (M) Michigan, (H) Huron, (E) Erie and (O) Ontario. Vertical dashed lines indicate the timings of seasonal maxima estimated by the "center of gravity" method. (a)—The months of *Chl-a* maximum estimated by the "center of gravity" method for each year in Lakes Superior, Michigan, Huron, Erie, and Ontario.

**Figure 10.** Maps of the month of maximum monthly median chlorophyll concentration estimated by the "center of gravity" method for the 'starting' (1998-2002; left column) and 'ending' (2018-2022; right column) five-year periods of the Ocean Colour Climate Change

Initiative (OC-CCI) dataset in Lakes Superior (S1, S2), Michigan (M1, M2), Huron (H1, H2), Erie (E1, E2) and Ontario (O1, O2).

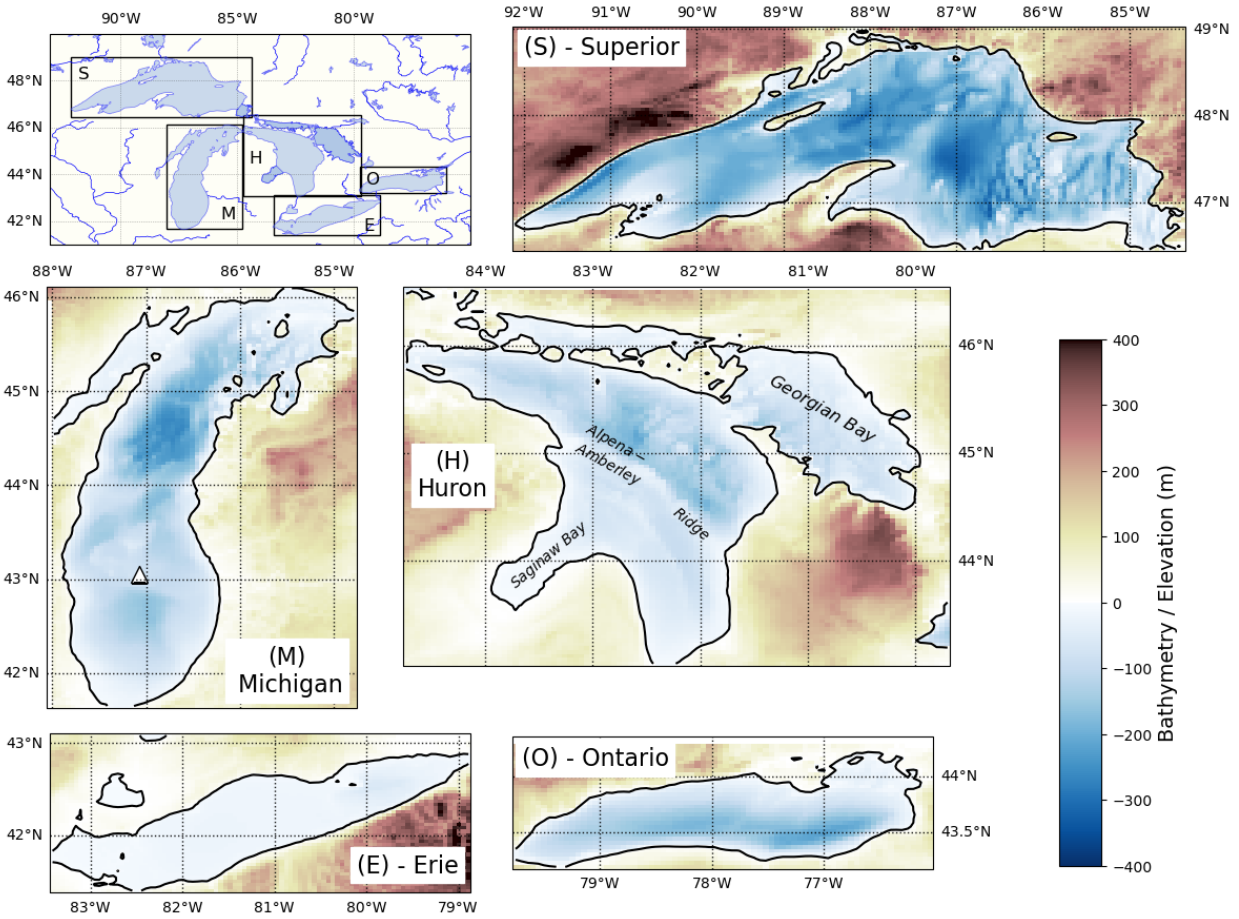


**Figure 1. Bathymetric maps of the Laurentian Great Lakes: (S) Superior, (M) Michigan, (H) Huron, (E) Erie, and (O) Ontario. Depth/elevation grids from https://www.ngdc.noaa.gov/mgg/greatlakes/. White triangle in (M) indicates the center (the location with maximum distance offshore) of Lake Michigan used later in Figures 2 and 3.**

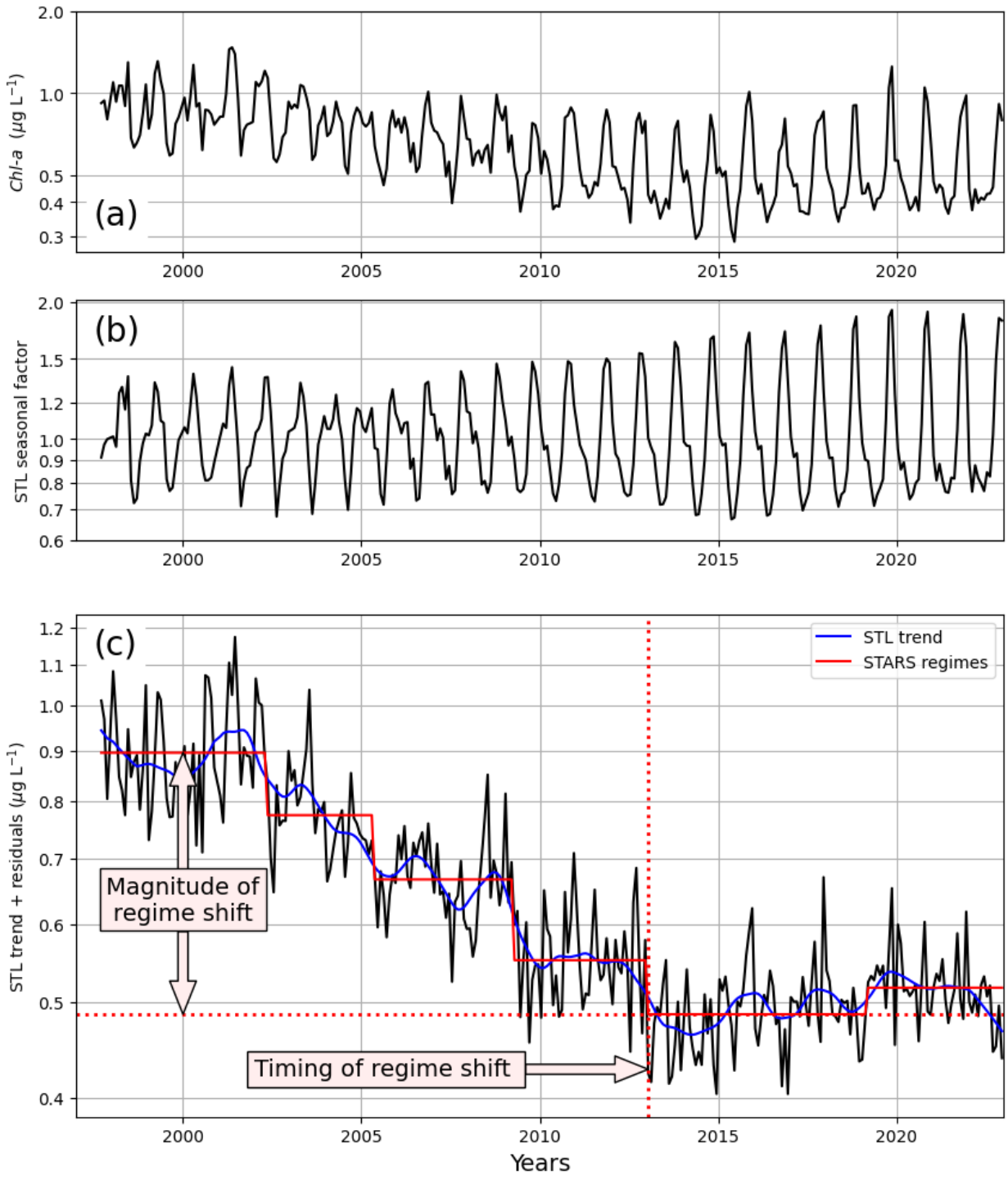


**Figure 2. An example of using (a) the time series of chlorophyll concentration (*Chl-a*; μg $L^{-1}$) in the center of Lake Michigan (latitude 43.047; longitude -87.070; depth 81 m; white triangle in Figure 1M) to determine the Seasonal-Trend decomposition using LOESS (STL). The *Chl-a* time series is split into the (b) seasonal factor (μg $L^{-1}$) and (c) smoothed trend (blue line; μg $L^{-1}$) and residuals (black line; μg $L^{-1}$). Regime shifts (solid red lines in (c)) are detected in the**

**"deseasonalized" time series (the sum of trend and residuals) using the Sequential T-test Analysis of Regime Shifts (STARS) method.**

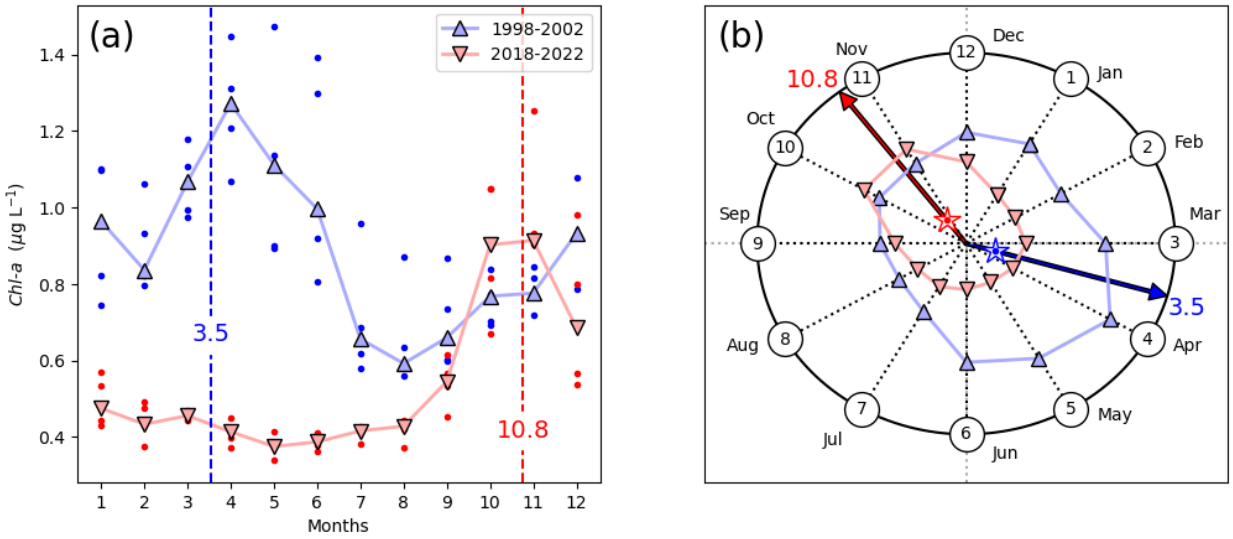


**Figure 3. (a)—Monthly median chlorophyll concentrations (dots) and its five-year median (filled triangles) in the center of southern Lake Michigan (white triangle in Figure 1M) for the initial (1998-2002; blue line; upward pointing triangles) and final (2018-2022; red line; downward pointing triangles) five-year periods of OC-CCI observations. (b)—Median monthly mean chlorophyll concentrations (blue polygon 1998-2002; red polygon 2018-2022) and the timings of annual maxima (arrows pointing through the centers of gravity represented by blue and red stars to the external circle representing a 12-month cycle) plotted in polar coordinates. The magnitude of average monthly median *Chl-a* is represented as the distance from the center of polar coordinates. In both 3a and 3b, the values of 3.5 and 10.8, indicate the timings in months of *Chl-a* maximum during 1998-2002 and 2018-2022, respectively.**

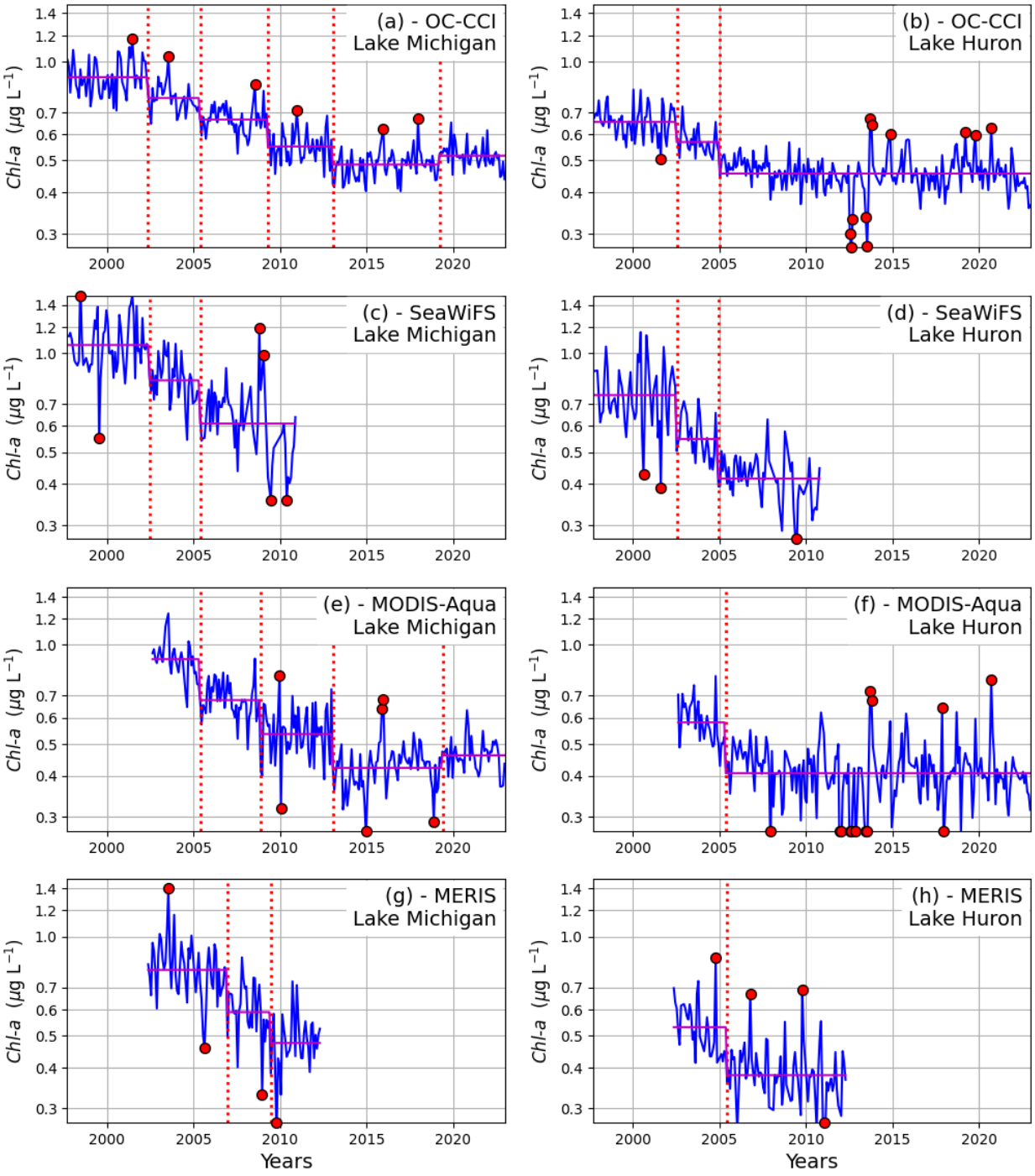


**Figure 4. Trends and regime shifts detected by the integrated STL-STARS method in median chlorophyll concentration (*Chl-a)* of (a, c, e, g) Lake Michigan and (b, d, f, h) Lake Huron based on observations of (a-b) OC-CCI, (c-d) SeaWiFS, (e-f) MODIS-Aqua, and (g-h) MERIS. Red circular markers indicate outliers, i.e., the values exceeding two standard deviations. Red dotted vertical lines indicate regime shifts; red horizontal lines indicate regime means.**

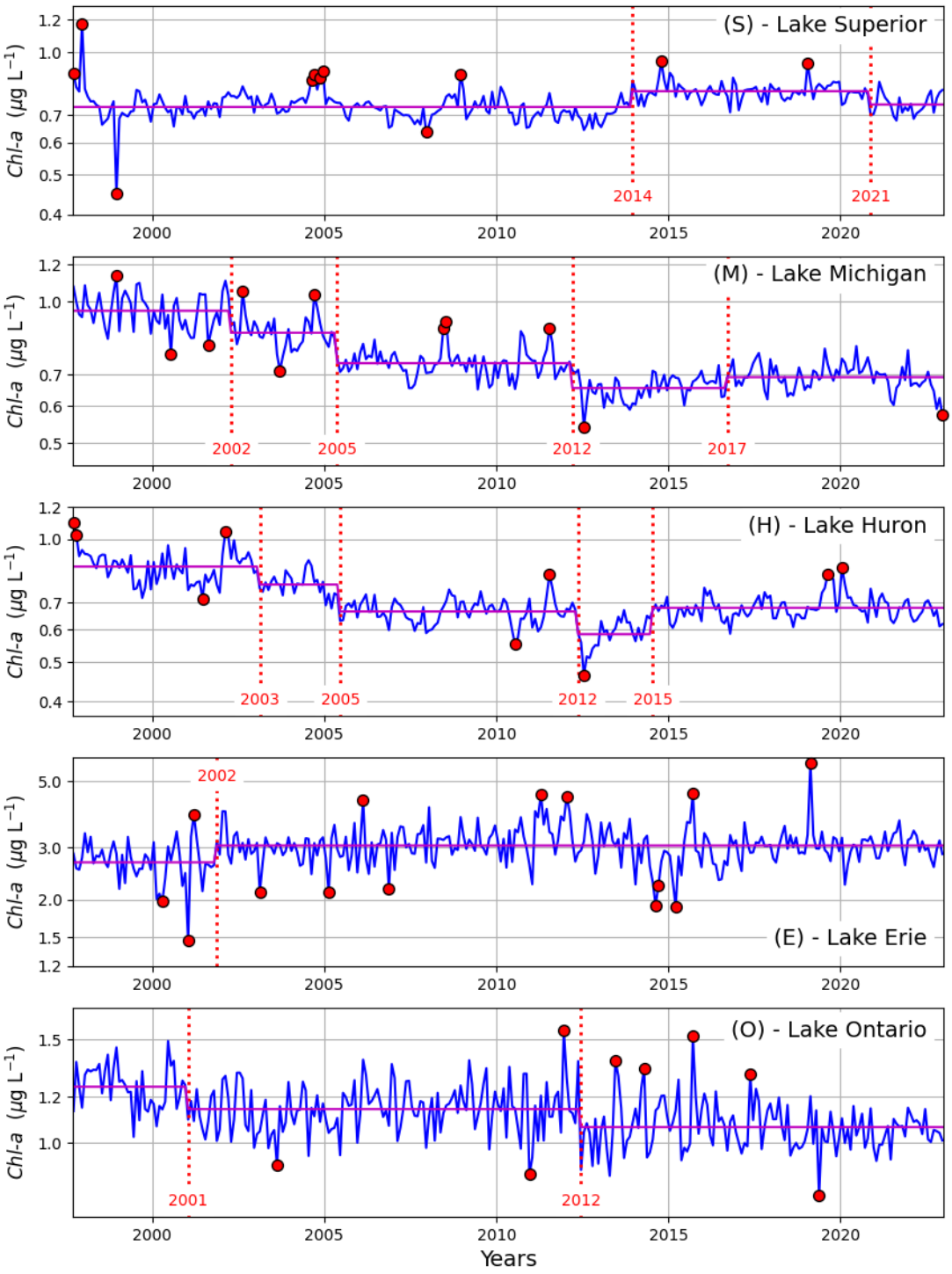


**Figure 5. Trends and regime shifts detected by the integrated STL-STARS method in OC-CCI median chlorophyll concentration (*Chl-a)* in Lakes (S) Superior, (M) Michigan, (H) Huron, (E) Erie and (O) Ontario. Red circular markers indicate outliers, i.e., the values exceeding two standard deviations. Red dotted vertical lines indicate regime shifts; red numbers indicate the years of regime shifts; red horizontal lines indicate regime means.**

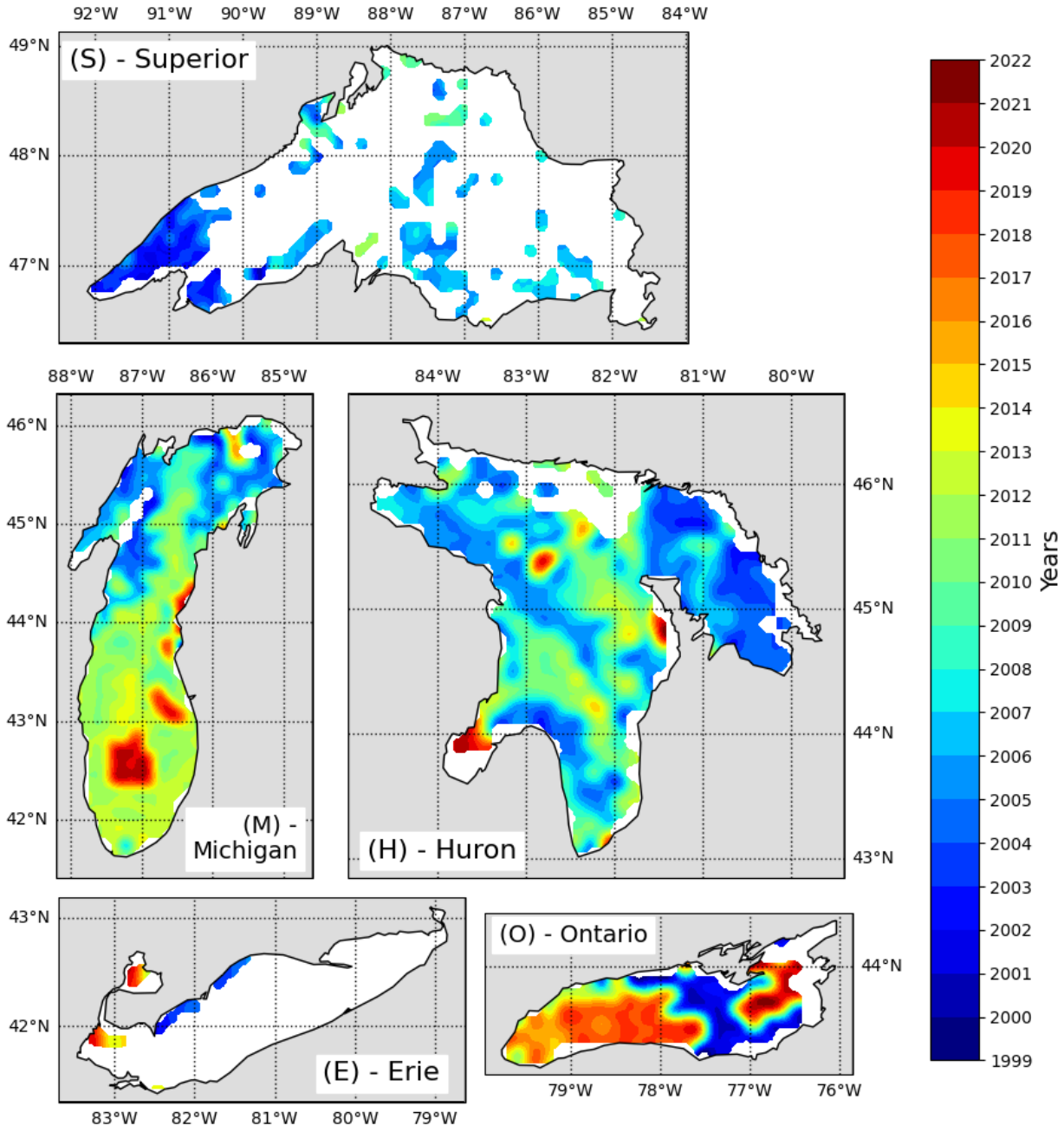


**Figure 6. Maps of the year in which chlorophyll concentrations (*Chl-a*) stabilized at a lower level in Lakes Superior (S), Michigan (M), Huron (H), Erie (E) and Ontario (O). White color indicates that no significant decrease in *Chl-a* was detected during the period (1997-2022) examined.**

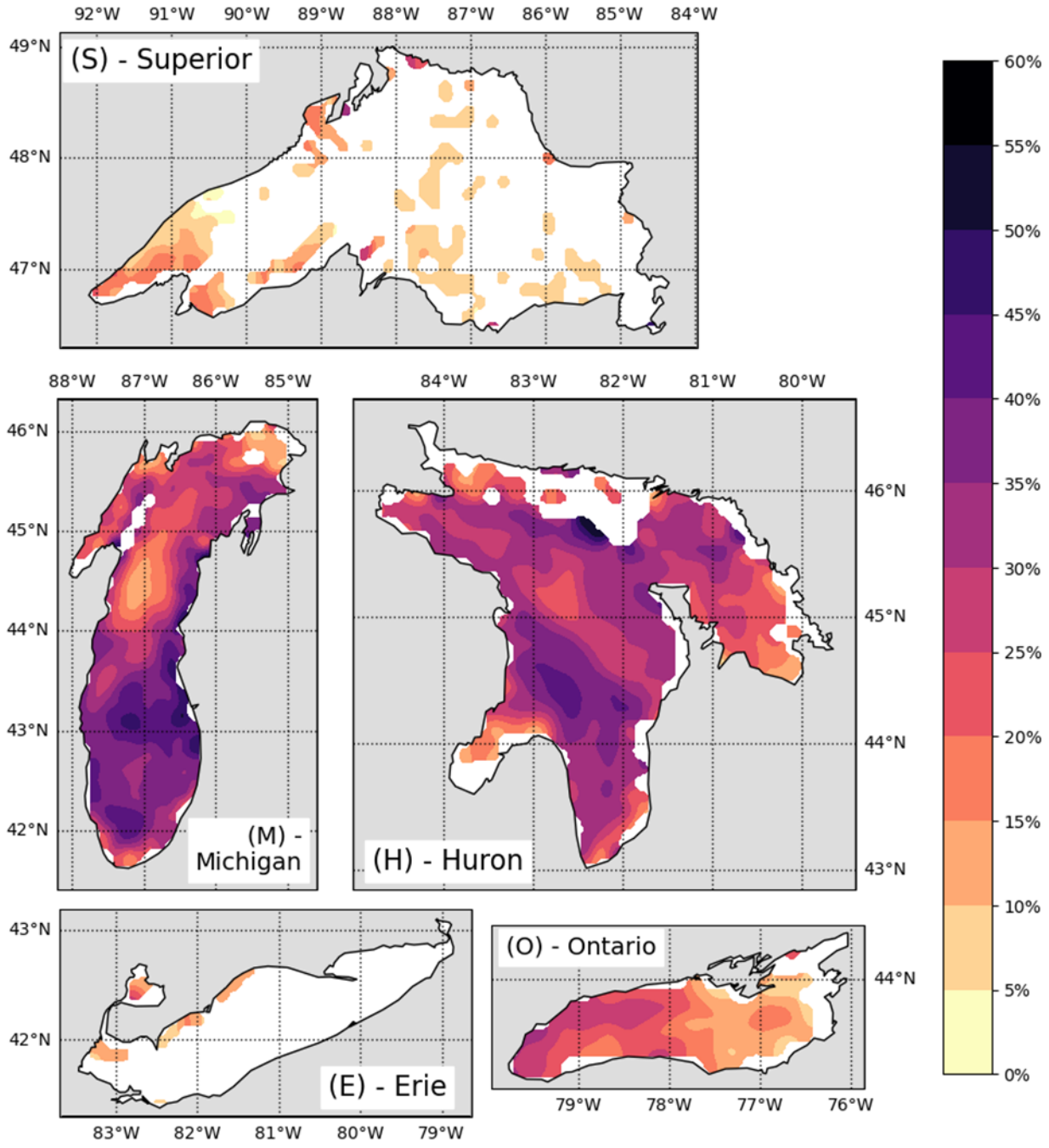


**Figure 7. Maps of the difference (in percent) of chlorophyll concentration (*Chl-a*) between the initial (starting 1997) and final (see Figure 6) regimes in Lakes Superior (S), Michigan (M), Huron (H), Erie (E) and Ontario (O). White color indicates that no significant decrease in *Chl-a* was detected during the period examined.**

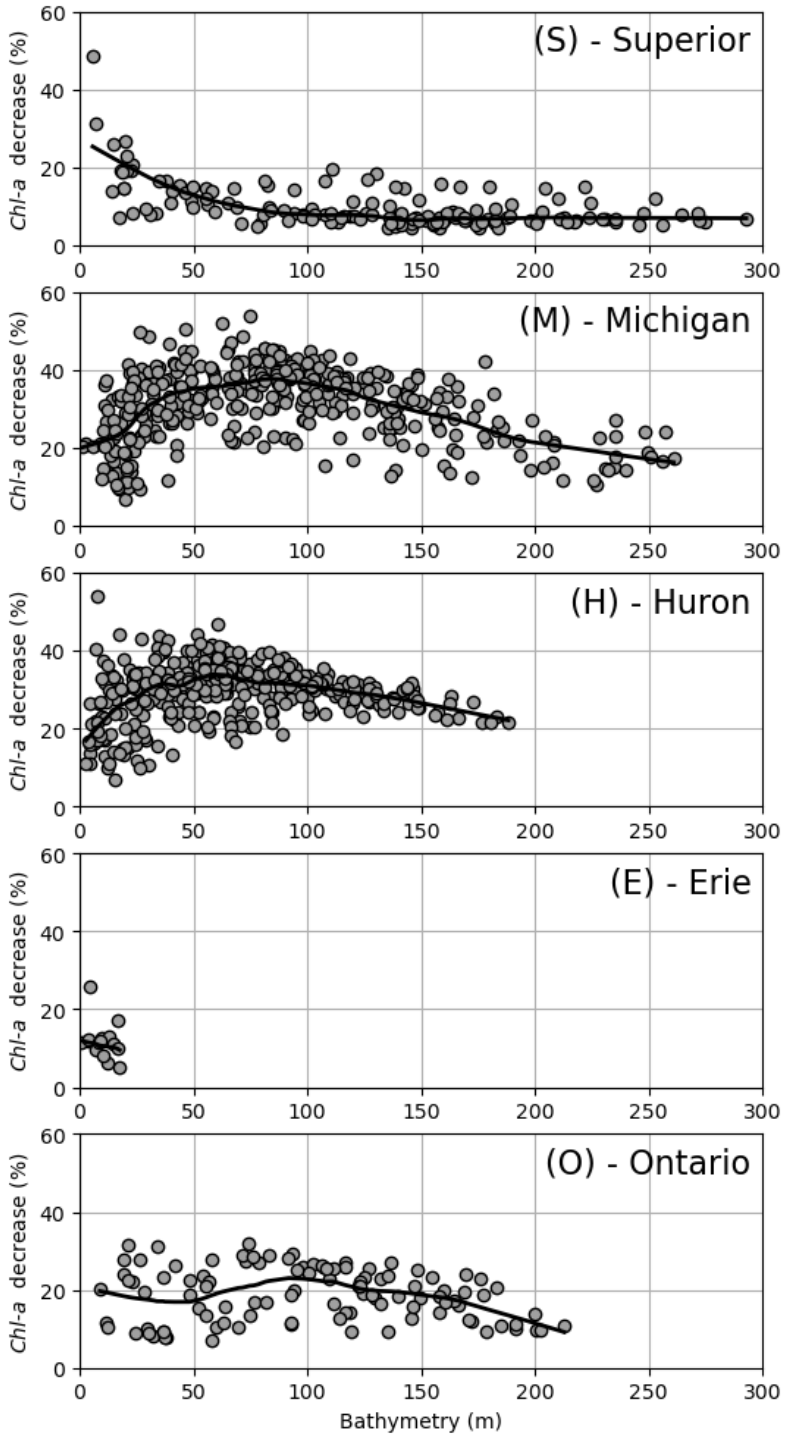


**Figure 8. Difference (in percent) of chlorophyll concentration (*Chl-a*) between the initial and final regimes (Figure 7) in relation to bathymetry in Lakes Superior (S), Michigan (M), Huron (H), Erie (E) and Ontario (O). The magnitudes of *Chl-a* decrease in 12-km grid cells (circles) were smoothed with LOESS function (black lines).**

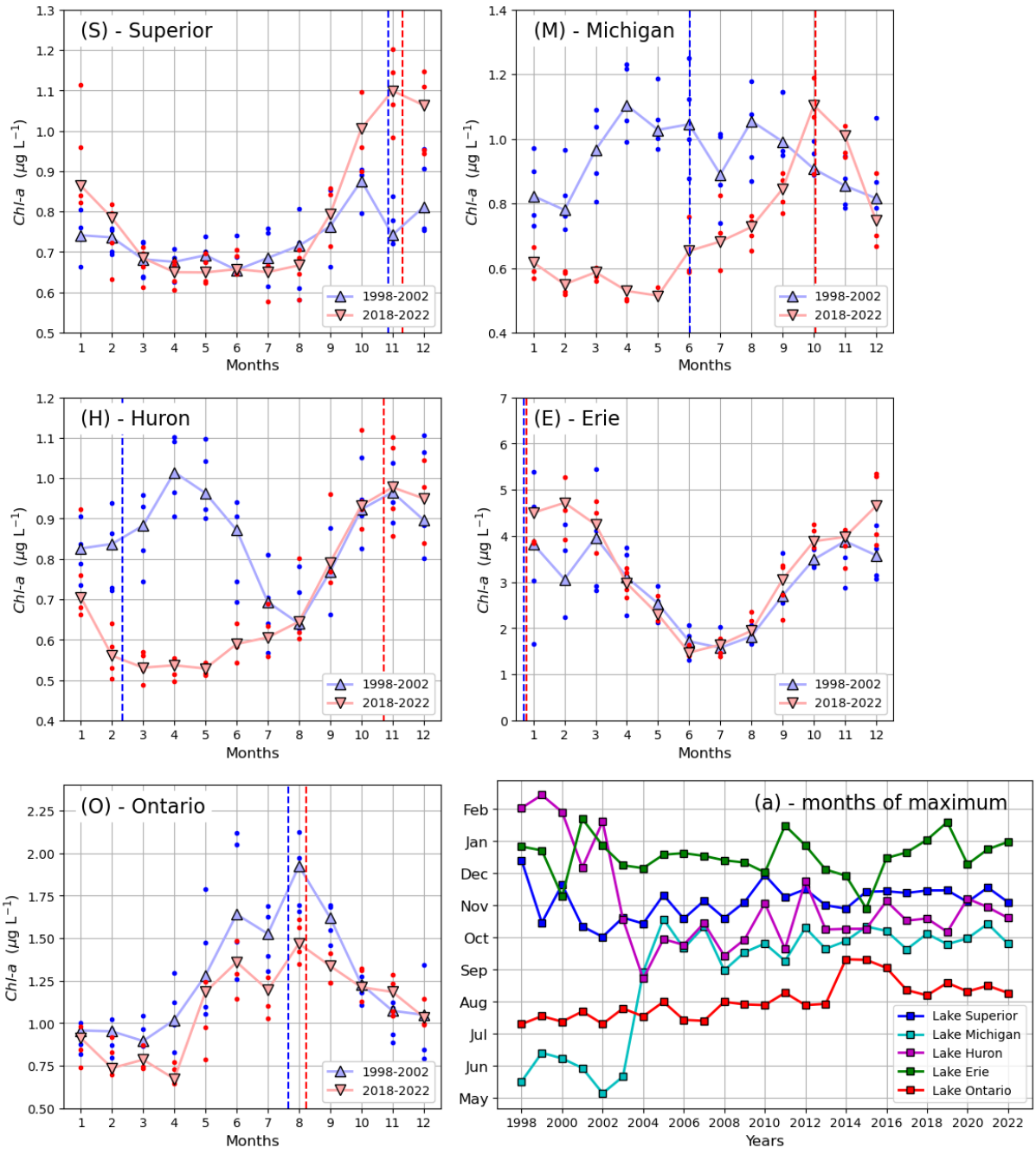


**Figure 9. Seasonal cycles of monthly median chlorophyll concentrations (*Chl-a*) in the initial (1998-2002; blue line; upward pointing triangles) and final (2018-2022; red line; downward pointing triangles) five-year periods of the Ocean Colour Climate Change Initiative (OC-CCI) dataset in Lakes Superior (S), Michigan (M), Huron (H), Erie (E) and Ontario (O). Vertical dashed lines indicate the timings of seasonal maxima estimated by the "center of gravity" method. (a)—The months of *Chl-a* maximum estimated by the "center of gravity" method for each year in Lakes Superior, Michigan, Huron, Erie, and Ontario (a).**

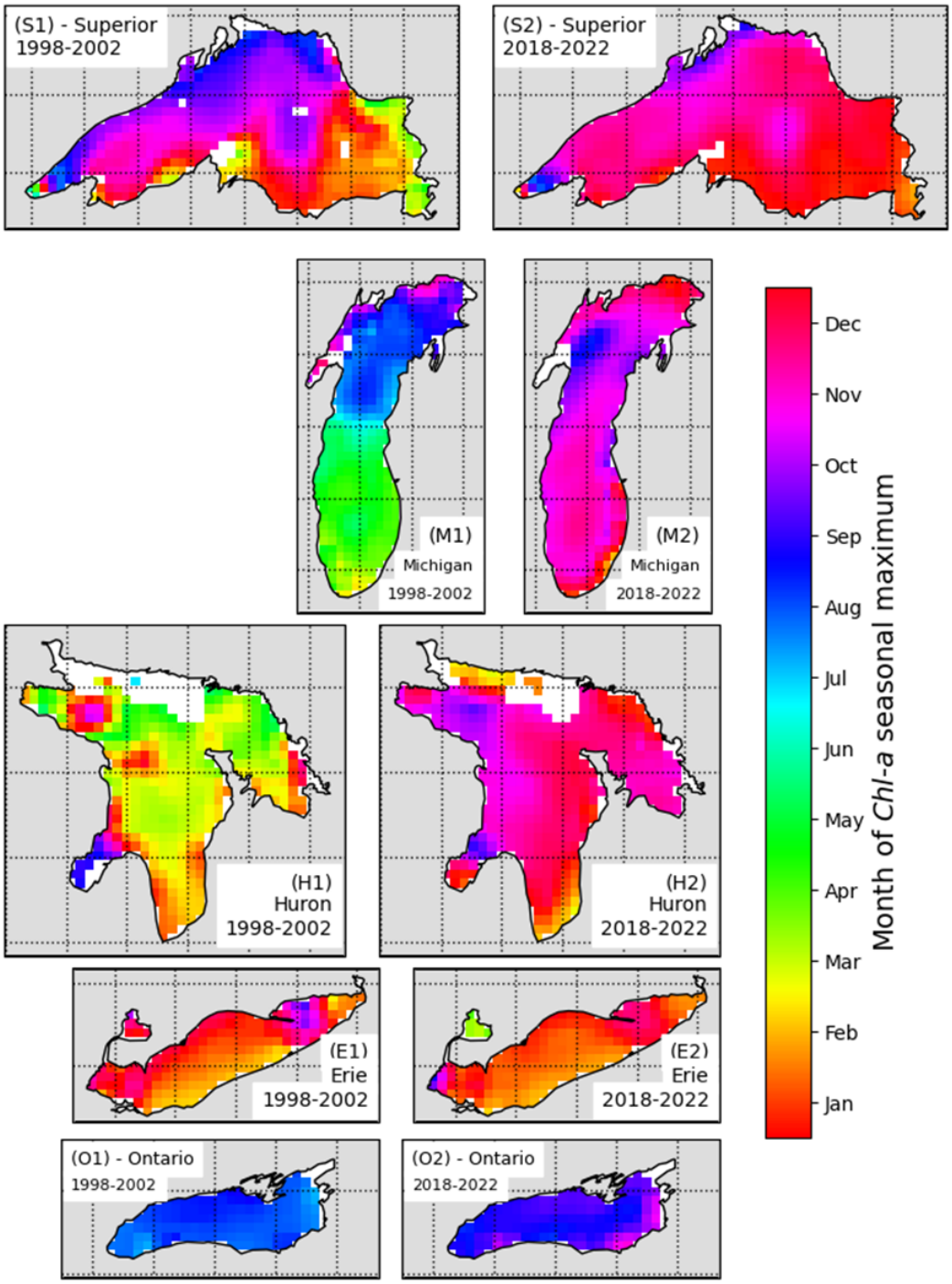


**Figure 10. Maps of the month of maximum monthly median chlorophyll concentration estimated by the "center of gravity" method for the initial (1998-2002; left column) and final (2018-2022; right column) five-year periods of the Ocean Colour Climate Change Initiative (OC-CCI) dataset in Lakes Superior (S1, S2), Michigan (M1, M2), Huron (H1, H2), Erie (E1, E2) and Ontario (O1, O2).**

**Supplementary materials to the manuscript:**

# Regime shifts in satellite-derived chlorophyll within the Laurentian Great Lakes

Nikolay P. Nezlin[1,2]*, SeungHyun Son[1,3], Christopher W. Brown[1,2,3], Prasanjit Dash[1,4],

Caren E. Binding[5], Ashley K. Elgin[6], Andrea VanderWoude[7]

[1] NOAA/NESDIS Center for Satellite Applications and Research, College Park, Maryland, USA

[2] Global Science & Technology, Inc., Greenbelt, Maryland, USA

[3] Cooperative Institute for Satellite Earth System Studies (CISESS)/Earth System Science Interdisciplinary Center (ESSIC), University of Maryland, College Park, MD, USA

[4] Cooperative Institute for Research in the Atmosphere (CIRA), Colorado State University, Fort Collins, Colorado, USA

[5] Environment and Climate Change Canada, Canada Centre for Inland Waters, Burlington, Ontario, Canada

[6] NOAA Great Lakes Environmental Research Laboratory, Lake Michigan Field Station, Muskegon, MI, USA

[7] NOAA Great Lakes Environmental Research Laboratory, Ann Arbor, MI, USA

*Corresponding author: nikolay.nezlin@noaa.gov; +1-(310)-770-1302

**Supplement 1. Colonization of the Laurentian Great Lakes by dreissenids**

The steps of colonization of dreissenids in the Great Lakes are described in publications (Karatayev et al., 2021; Karatayev & Burlakova, 2022; Nalepa et al., 2010, 2009; Strayer et al., 2019). Figures S1a and S1b (source: Fig. 3 and Fig. 6 from Lake morphometry determines Dreissena invasion dynamics, Karatayev et al., Biological Invasions, Volume 23, Springer Nature, 2021, reproduced with permission from SNCSC) demonstrate how the two species of mussels (zebra mussels at upper panels and quagga mussels at lower panels) spread across the entire bottom of shallow (Figure S1a) and deep (Figure S1b) basins.

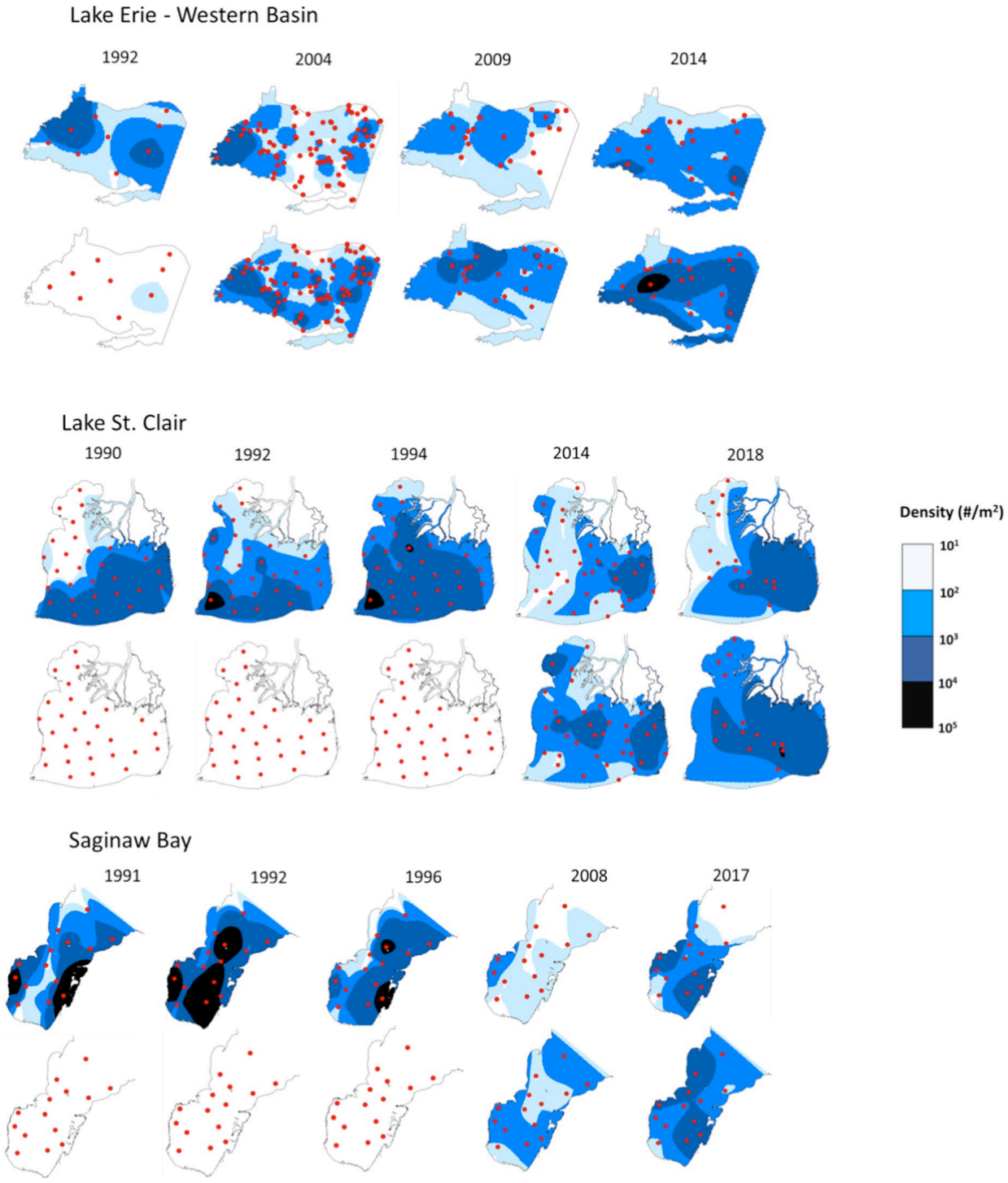


**Figure S1a. Source: Fig. 3 from (Lake morphometry determines Dreissena invasion dynamics, Karatayev et al., Biological Invasions, Volume 23, Springer Nature, 2021, reproduced with permission from SNCSC). Spatial distribution of *Dreissena polymorpha* (upper rows within each lake panel) and *D. rostriformis bugensis* (lower rows) in shallow lakes/regions of Lake Erie-Western Basin, Lake St. Clair, and Huron Lake-Saginaw Bay. Dreissenid density is expressed as individuals $m^{-2}$. Red dots indicate sampling stations.**

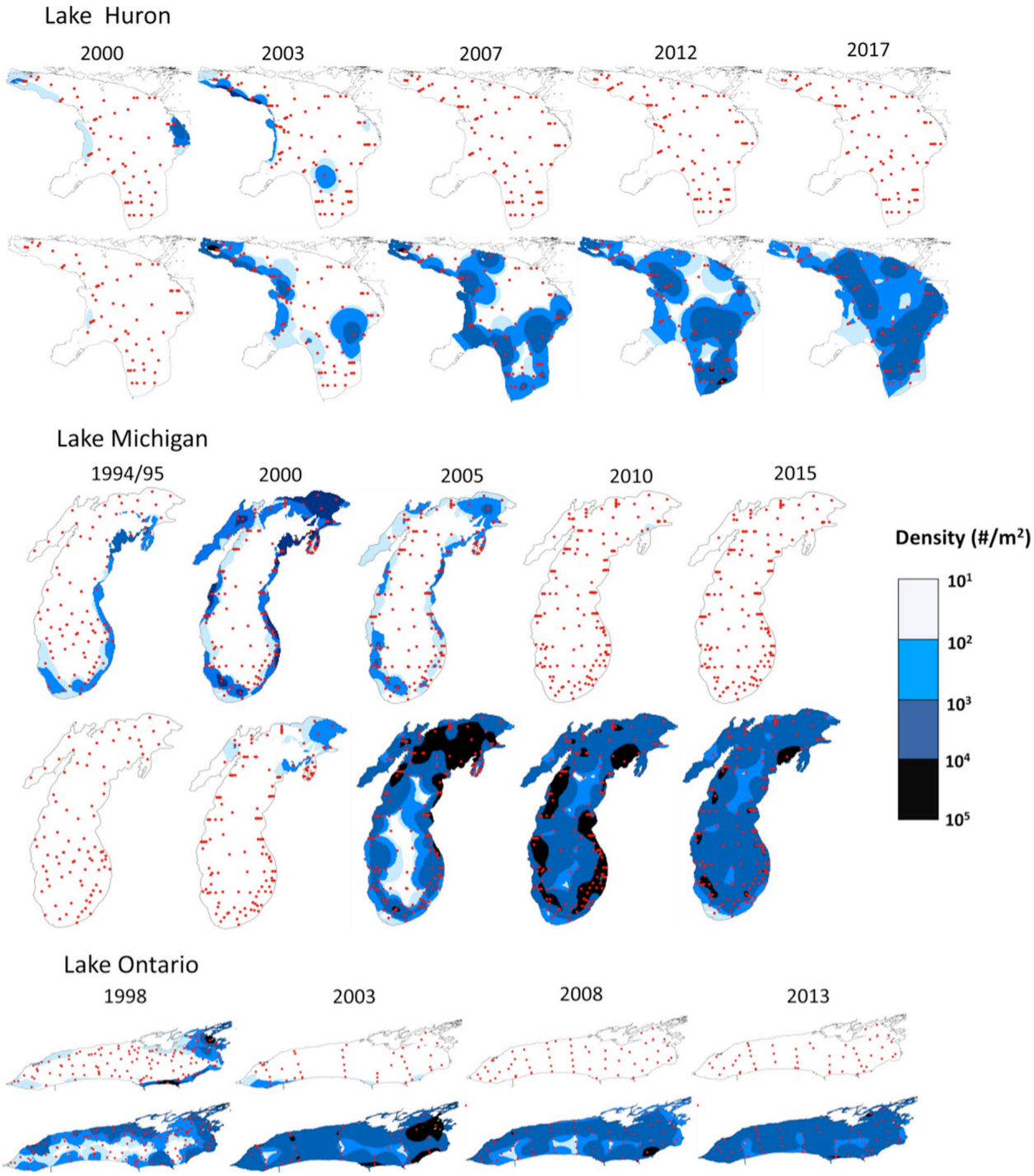


**Figure S1b. Source: Fig. 6 from (Lake morphometry determines Dreissena invasion dynamics, Karatayev et al., Biological Invasions, Volume 23, Springer Nature, 2021, reproduced with permission from SNCSC). Spatial distribution of *Dreissena polymorpha* (upper rows within each lake panel) and *D. rostriformis bugensis* (lower rows) in deep Lake Huron, Lake Michigan, and Lake Ontario. Dreissenid density is expressed as individuals $m^{-2}$. Red dots indicate sampling stations.**

**Supplement 2. Inter-mission differences and biases between satellite sensors misinterpreted as regime shifts**

Although in the OC-CCI dataset the biases between the data collected by different satellites were corrected, a significant number of artifacts remained and could be misinterpreted as regime shifts. However, OC-CCI *Chl-a* data reveal the basic patterns of regime shifts in the Great Lakes because the scale of these transformations is higher than the differences between bias-corrected *Chl-a* collected by different satellites.

The chance to detect regime shifts (both positive and negative) by STARS algorithm in all cells of 12-km grids in each of the five lakes demonstrate four maxima: in 2002, 2005, 2013 and 2020 (Figure S2b), and three of them coincide with the periods when the sources of data from satellite sensors integrated in the OC-CCI dataset changed (Figure S2a). Specifically, in 2002, SeaWiFS had been operational for five years when MODIS-Aqua and MERIS were launched, and the total number of collected images dramatically increased. From 2012 to 2013, MERIS ceased operations, and VIIRS-SNPP was launched. Starting in 2020, MODIS-Aqua and VIIRS-SNPP were not used in the OC-CCI dataset due to sensor degradation problems. These periods of changes in the origin of satellite data used in the OC-CCI dataset resulted in *Chl-a* discontinuities remaining after bias-correction procedures (Garnesson et al., 2019; Hammond et al., 2018; Yu et al., 2023) and could be misinterpreted as regime shifts.

The highest number of regime shifts in 2013 (when MERIS was replaced by SNPP VIIRS) and 2020 (when MODIS-Aqua and VIIRS-SNPP ceased being used) was detected in Lake Superior (gray bars in Figure S2b), where no regime transformation took place and all detected regime shifts should be treated as artifacts.

It is worth mentioning that some periods when the chance to detect regime shift in the Great Lakes was higher than during other years had reasonable explanations not necessarily associated with the change of sensors. In 2011-2013, the change in observing satellites (MERIS replaced by SNPP VIIRS) coincided with extreme weather conditions. After warm winter of 2011–2012, late winter cooling and an early spring warming resulted in incomplete fall overturning facilitating cross-shelf circulation delay, reducing deep-water ventilation and limiting the supply of nutrients to the sunlit surface layers (Fichot et al., 2019). During the next winter 2012-2013, the Great Lakes endured the most persistent, lowest temperatures and highest ice cover in recent history (Gronewold et al., 2015), which could result in discontinuities in *Chl-a* time series. The period 2004-2005 was noted by other authors as a point when the most dramatic drop in water quality parameters occurred in the Great Lakes, including a decrease of water turbidity in Lakes Michigan and Huron (Zheng & DiGiacomo, 2022) and a decline in phytoplankton biomass in the southern basin of Lake Michigan (Reavie et al., 2014).

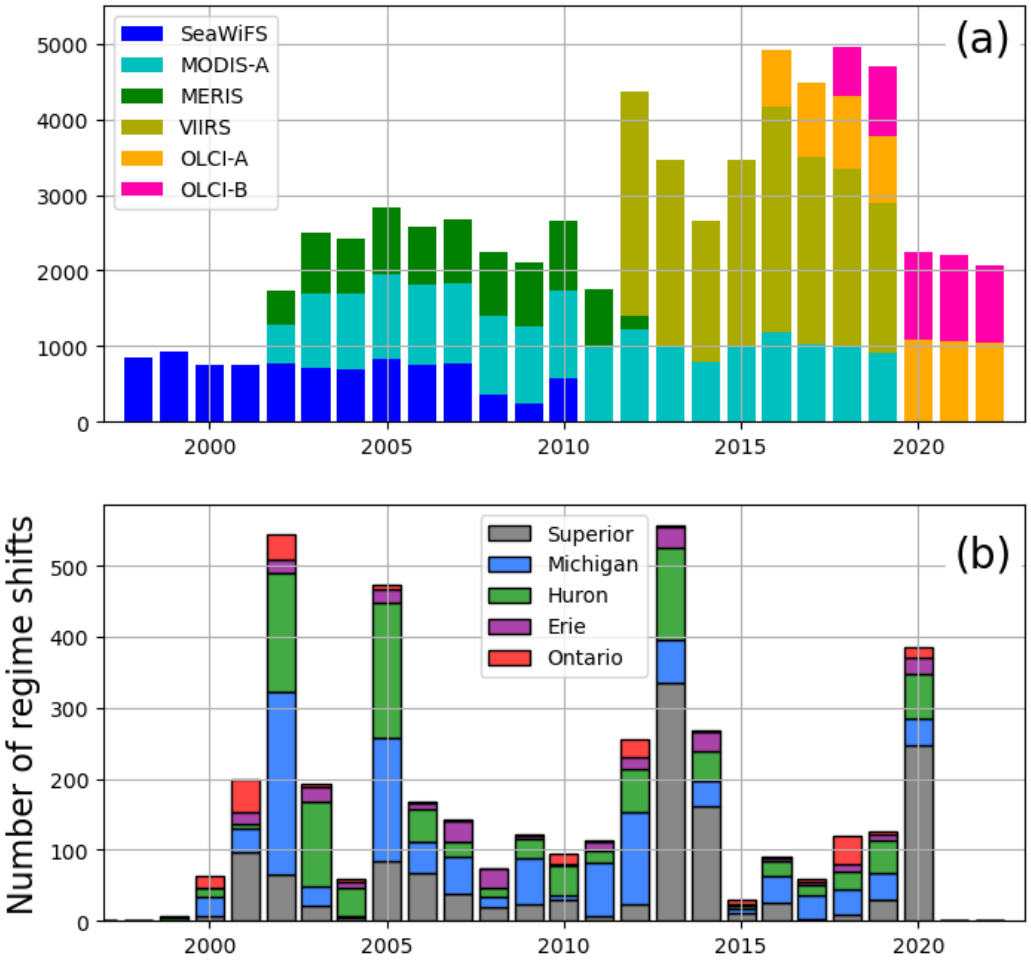


**Figure S2. The relationship between (a) the number of images collected over the Great Lakes by different satellite sensors used in the OC-CCI dataset and (b) the number of regime shifts (both positive and negative) detected by the integrated STL-STARS method during every year in all grid cells of the five Great Lakes.**

**Supplement 3. Different number of images collected during different seasons**

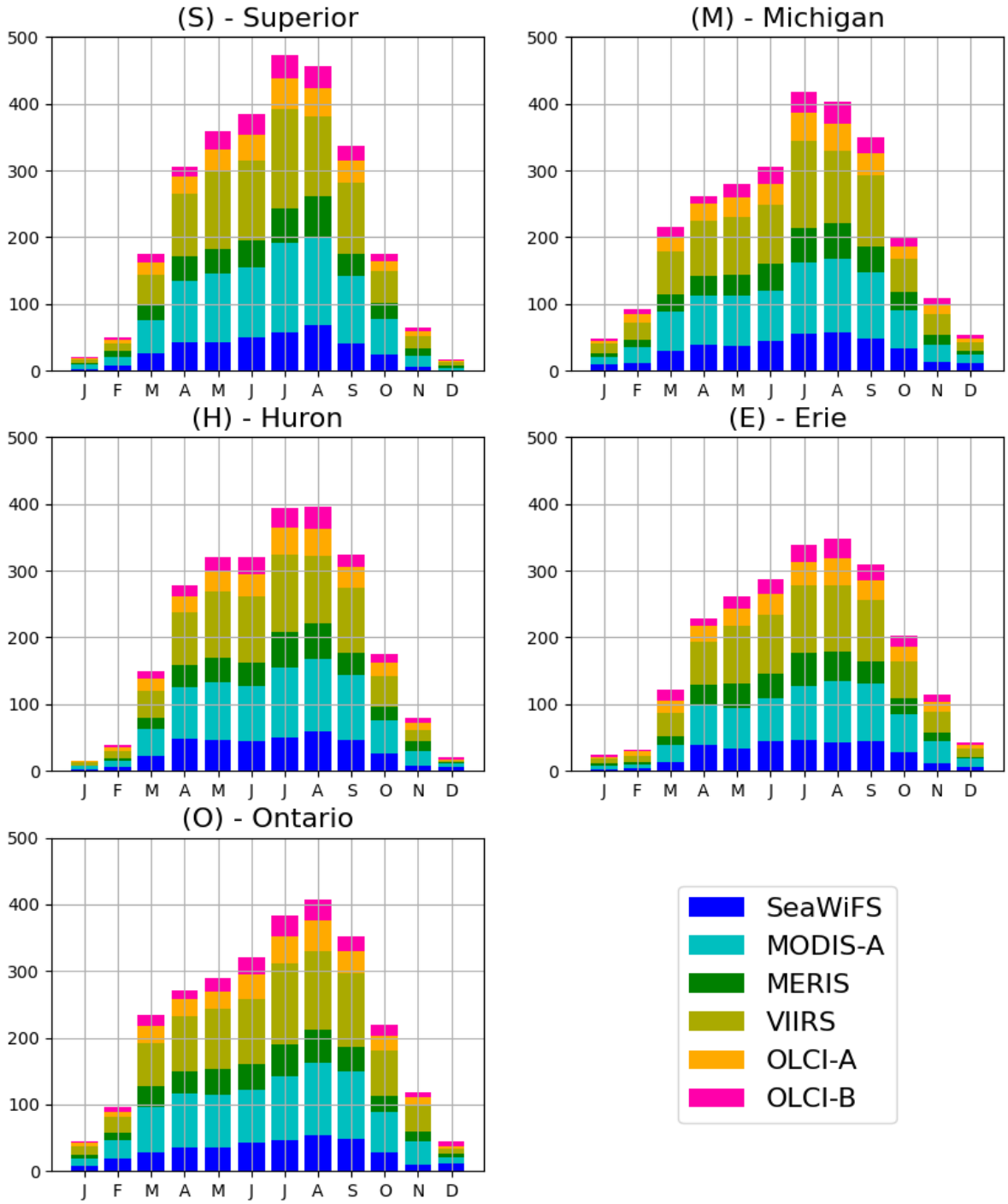


**Figure S3. The mean numbers of images collected over the lakes Superior (S), Michigan (M), Huron (H), Erie (E), and Ontario (O) by different satellite sensors used in the OC-CCI dataset during different months.**

**Supplement 4. Preliminary comparison between in-situ and satellite *Chl-a* measurements in the Great Lakes.**

At the preliminary step preceding this study, we compared in-situ *Chl-a* measurements in the Great Lakes from Environmental Protection Agency (EPA) Great Lakes Environmental Database System (GLENDA) with VIIRS-SNPP Level-2 *Chl-a* products using OC3V algorithm (at 1×1 km spatial resolution) from 2018 to 2023. The matchup comparison is shown in the following Figure S4. As mentioned, VIIRS OC3V *Chl-a* data are underestimated, but more systematically.

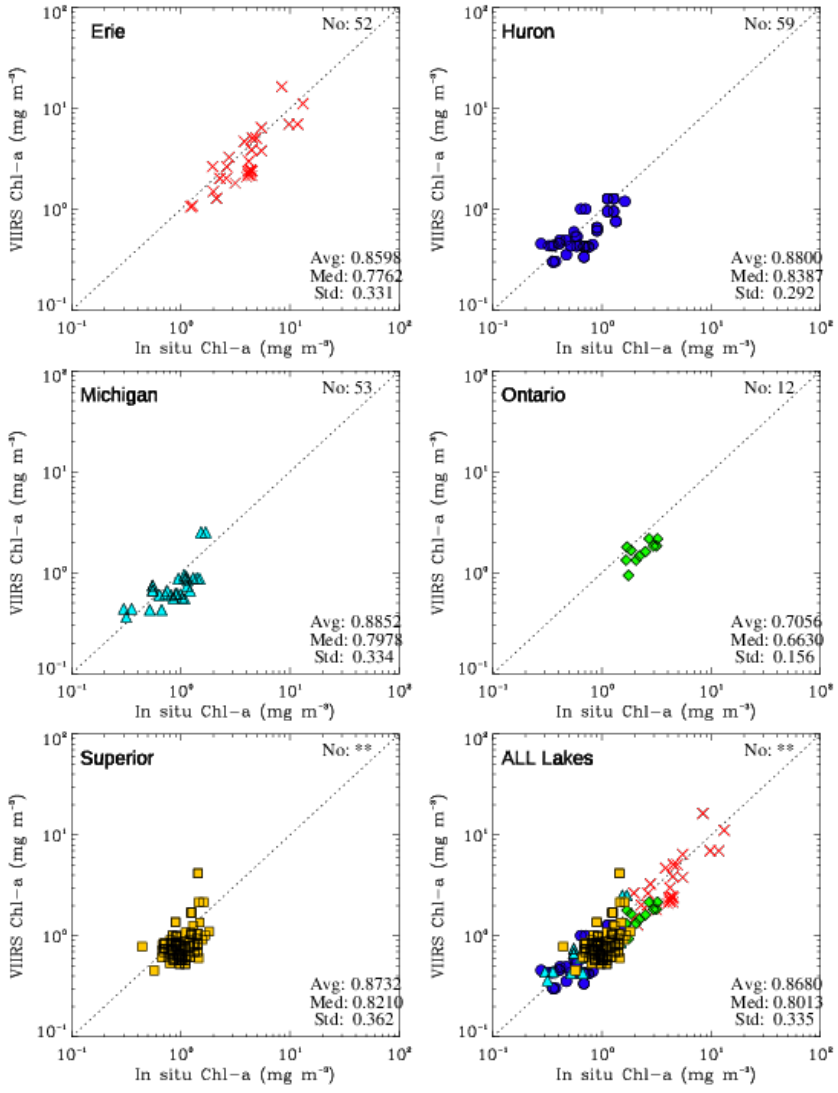


**Figure S4. Comparison between in-situ and satellite *Chl-a* measurements in the Great Lakes.**

## References


Fichot, C. G., Matsumoto, K., Holt, B., Gierach, M. M., & Tokos, K. S. (2019). Assessing change in the overturning behavior of the Laurentian Great Lakes using remotely sensed lake surface water temperatures. Remote Sens. of Environ., 235, 111427. https://doi.org/https://doi.org/10.1016/j.rse.2019.111427

Garnesson, P., Mangin, A., Fanton d'Andon, O., Demaria, J., & Bretagnon, M. (2019). The CMEMS GlobColour chlorophyll a product based on satellite observation: multi-sensor merging and flagging strategies. Ocean Science, 15(3), 819-830. https://doi.org/10.5194/os-15-819-2019

Gronewold, A. D., Anderson, E. J., Lofgren, B., Blanken, P. D., Wang, J., Smith, J., Hunter, T., Lang, G., Stow, C. A., Beletsky, D., & Bratton, J. (2015). Impacts of extreme 2013–2014 winter conditions on Lake Michigan's fall heat content, surface temperature, and evaporation. Geophysical Res. Letters, 42(9), 3364-3370. https://doi.org/10.1002/2015GL063799

Hammond, M. L., Beaulieu, C., Henson, S. A., & Sahu, S. K. (2018). Assessing the Presence of Discontinuities in the Ocean Color Satellite Record and Their Effects on Chlorophyll Trends and Their Uncertainties. Geophysical Res. Letters, 45(15), 7654-7662. https://doi.org/10.1029/2017GL076928

Karatayev, A., Karatayev, V., Burlakova, L., Mehler, K., Rowe, M., Elgin, A., & Nalepa, T. (2021). Lake morphometry determines Dreissena invasion dynamics. Biological Invasions, 23, 2489–2514. https://doi.org/10.1007/s10530-021-02518-3

Karatayev, A. Y., & Burlakova, L. E. (2022). Dreissena in the Great Lakes: what have we learned in 30 years of invasion. Hydrobiologia. https://doi.org/10.1007/s10750-022-04990-x

Nalepa, T. F., Fanslow, D. L., & Lang, G. A. (2009). Transformation of the offshore benthic community in Lake Michigan: recent shift from the native amphipod Diporeia spp. to the invasive mussel *Dreissena rostriformis bugensis*. Freshw. Biology, 54(3), 466-479. https://doi.org/10.1111/j.1365-2427.2008.02123.x

Nalepa, T. F., Fanslow, D. L., & Pothoven, S. A. (2010). Recent changes in density, biomass, recruitment, size structure, and nutritional state of Dreissena populations in southern Lake Michigan. J. of Great Lakes Res., 36, 5-19. https://doi.org/10.1016/j.jglr.2010.03.013

Reavie, E. D., Barbiero, R. P., Allinger, L. E., & Warren, G. J. (2014). Phytoplankton trends in the Great Lakes, 2001–2011. J. of Great Lakes Res., 40(3), 618-639. https://doi.org/10.1016/j.jglr.2014.04.013

Strayer, D. L., Adamovich, B. V., Adrian, R., Aldridge, D. C., Balogh, C., Burlakova, L. E., Fried-Petersen, H. B., G.-Tóth, L., Hetherington, A. L., Jones, T. S., Karatayev, A. Y., Madill, J. B., Makarevich, O. A., Marsden, J. E., Martel, A. L., Minchin, D., Nalepa, T. F., Noordhuis, R., Robinson, T. J., . . . Jeschke, J. M. (2019). Long-term population dynamics of dreissenid

mussels (*Dreissena polymorpha* and *D. rostriformis*): a cross-system analysis. Ecosphere, 10(4), e02701. https://doi.org/10.1002/ecs2.2701

Yu, S., Bai, Y., He, X., Gong, F., & Li, T. (2023). A new merged dataset of global ocean chlorophyll-a concentration for better trend detection [Original Research]. Frontiers in Marine Science, 10. https://doi.org/10.3389/fmars.2023.1051619

Zheng, G., & DiGiacomo, P. M. (2022). A simple water clarity-turbidity index for the Great Lakes. J. of Great Lakes Res., 48(3), 686-694. https://doi.org/10.1016/j.jglr.2022.03.005